Journal
of
The Franklin Institute

EDITOR, HENRY BUTLER ALLEN, MET.E., D.SC.
EDITORIAL ASSISTANT, NANCY S. GLENN, M.A.

Associate Editors:

WILDER D. BANCROFT, PH.D. — C. B. BAZZONI, PH.D. — ARTHUR L. DAY, SC.D. — R. EKSERGIAN, PH.D. — PAUL D. FOOTE, PH.D. — W. J. HUMPHREYS, PH.D. — C. E. K. MEES, D.SC. — WILLIAM B. MELDRUM, PH.D. — HENRY C. SHERMAN, SC.D. — W. F. G. SWANN, D.SC. — HUGH S. TAYLOR, D.SC. — A. F. ZAHM, PH.D. — JOHN ZELENY, PH.D.

Committee on Publications:

G. H. CLAMER, CHAIRMAN — RICHARD HOWSON — C. L. JORDAN — LIONEL F. LEVY — MALCOLM LLOYD, JR. — HIRAM S. LUKENS — RICHARD H. OPPERMANN — WINTHROP R. WRIGHT

Vol. 246 **NOVEMBER, 1948** **No. 5**

CONTENTS

A Study of Chemically Deposited Silver Mirrors. RAYMOND MORGAN AND RALPH D. MYERS 363

Electron Lenses of Hyperbolic Field Structure. Part II..... REINHOLD RÜDENBERG 377

Optimum Ratio Between Crank Arm and Connecting Rod for Smooth Operation of Reciprocating Engines..... W. S. KIMBALL 409

Notes from The National Bureau of Standards..... 419

The Franklin Institute
- Medal Day Meeting..... 425
- Committee on Science and the Arts..... 426
- Museum Notes..... 427
- Library Notes..... 427
- Book Reviews..... 428

Notes from The Biochemical Research Foundation..... 435
- Manometric Determination of Carboxypeptidase..... CHARLES A. ZITTLE

Current Topics..... 438

Published at
Prince and Lemon Streets, Lancaster, Penna., by
THE FRANKLIN INSTITUTE OF THE STATE OF PENNSYLVANIA
Benjamin Franklin Parkway at Twentieth St., Philadelphia 3, Penna.

DOMESTIC—EIGHT DOLLARS PER YEAR FOREIGN—NINE DOLLARS PER YEAR
(Foreign Postage Additional)
SINGLE CURRENT NUMBERS—ONE DOLLAR EACH
REPRINTS—FIFTY CENTS PER INDIVIDUAL INSTALLMENTS

Indexes to the semi-annual volumes of the JOURNAL are published with the June and December numbers

PHILCO

Famous for Quality

the World Over

RADIOS • PHONOGRAPHS • FM • TELEVISION

REFRIGERATORS • FREEZERS • AIR CONDITIONERS

Journal
of
The Franklin Institute
Devoted to Science and the Mechanic Arts

Vol. 246 NOVEMBER, 1948 No. 5

A STUDY OF CHEMICALLY DEPOSITED SILVER MIRRORS.

BY

RAYMOND MORGAN[1] AND RALPH D. MYERS.[1]

INTRODUCTION.

The production of silver mirrors by the chemical deposition of the metal on glass has become an art rather well developed by industry. Thousands of square feet are produced daily; nevertheless a knowledge of the nature of the chemical and physical actions is rather limited.

The object of this research was to study the nature of mirrors produced by various methods in order to gain information, particularly on: (1) the structure of the silver coatings; (2) the presence of impurities in the coatings; and (3) the associated chemical compounds in the cases of spoilage.

At present, there are used commercially modifications of three processes; (1) the Rochelle Epsom Salts, hot table process; (2) the Weber, cold pouring process; and (3) the spray method using hydrazine compound as a reducer for silver ammonia nitrate solution.

The spray process from the standpoint of mass production is much to be desired. However, the quality of the mirrors produced by this method has been thought by some to be inferior.

In particular it has been contended:

1. A mirror produced by the spray method exhibits less adhesion to the glass.
2. Spoilage is more conspicuous in mirrors produced by this method.
3. There is a difference in the reflectivity of the silver coating.

The spray process is very rapid and there is a question as to whether either the size of the particle or the structure of the silver mirror film

[1] Department of Physics, University of Maryland, College Park, Md.

(Note—The Franklin Institute is not responsible for the statements and opinions advanced by contributors in the JOURNAL.)

varies basically with the speed of precipitation. Also, do the mirrors differ chemically due to the inclusion of impurities?[2]

In the production of silver mirrors, the glass surface is usually sensitized by the use of stannous chloride before the deposition of the mirror. There has been no exhaustive study of what happens in the use of the sensitizer. It plays a most important part in the production of mirrors. As a matter of fact, it is difficult to produce good commercial mirrors without the use of the sensitizer.

Extensive work on silver mirrors was done by V. Kohlshutter and E. Fishchmann (1).[3] However, the technique of the methods that they employed was not suitable for determining the physical nature of the silver films. Kohlshutter concluded that the surface adjacent to the glass consisted of colloidal silver and was amorphous in nature. As to the nature of colloidal silver, P. v. Scherrer (2) describes work on colloidal systems of silver which were found to crystallize with the same atomic arrangement that prevails in the macrocrystalline metal. Wartenberg (3) studied the effect of the sensitizing agent and concluded that in the silver process, the oxidizing agents have no effect on the efficiency of the sensitizing solution.

PROCEDURE.

Use was made principally of X-ray and electron diffraction. The electron diffraction patterns were made of thin films by allowing the beam to pass through the film and of surfaces by allowing the beam to strike the surface at grazing incidence. For convenience we shall refer to the first as patterns by transmission and to the second as patterns by reflection. A number of other techniques, also, were employed to a limited extent such as: (1) adhesion of the silver to the glass; (2) optical constants of the glass-silver interface; (3) spectrum analysis; (4) influence of certain corroding agents; and (5) effect of aging the mirrors in a vacuum in the presence of an active drying agent.

The following formulae were used for silvering:

Hot Table Process.

Solution 1.

454	g.	Silver Nitrate, Peacock Lab., Inc., c.p.
355	ml.	Ammonium Hydroxide, 28.42 per cent, Bakers, c.p.
5.45	l.	Distilled Water

Dissolve the silver nitrate crystals in the water. Add ammonium

[2] Extensive work has been done on the inclusion of extraneous materials in electroplated silver, particularly by G. A. Hulett and T. W. Richards with the silver voltameter. The extraneous materials found included in the case of silver mirrors chemically deposited on glass are enormously greater than found in the case of electroplated silver films.

[3] The boldface numbers in parentheses refer to the references appended to this paper.

hydroxide slowly with stirring, filter clear, and store in clean glass bottle.

Solution 2.

1590	g.	Rochelle Salt, Merck's U.S.P.
114	g.	Magnesium Sulfate, Merck's U.S.P.
3.64	l.	Distilled Water

Dissolve the chemicals in water and filter the solution. Store in a clean glass bottle.

When ready to pour mirrors, mix:

256	ml.	Solution 1
256	ml.	Solution 2
3.64	l.	Distilled Water

and pour on glass which has been leveled on the heated silvering table.

Cold Pouring Process.

Solution 1.

114	ml.	95 per cent Pure Grain Alcohol
114	ml.	Distilled Water
14.2	ml.	Sulfuric Acid, sp. gr. 1.84, Bakers, c.p.

Solution 2.

14.2	ml.	Solution 1
1.14	l.	Distilled Water

Bring to boil in glass container and add:

114	g.	Rock Candy, Merck's

Boil 10 min.

Solution 3.

21.6	l.	Distilled Water
114	g.	Sodium Hydroxide, 95 per cent Merck's U.S.P.

Dissolve thoroughly.

Solution 4.

1.14	l.	Distilled Water
128	g.	Silver Nitrate, Peacock Lab., Inc., c.p.
398	ml.	Ammonium Hydroxide, 28.42 per cent, Bakers, c.p.

Dissolve the silver nitrate in the water, add the ammonium hydroxide while stirring, and filter clear; store in a clean bottle.

Solution 5.

Mix equal volumes of solutions 3 and 4, always pouring 3 into 4. (This solution should *not* be stored—explosion may result.) When

ready to make mirrors: mix 3.55 ml. of solution 2 with 568 ml. of solution 5 and pour on glass prepared for silvering. In carrying out the entire process, great care should be taken to prevent explosion, especially on hot days.

Spray Process.

Solution 1.

114	g.	Silver Nitrate, Peacock Lab., Inc., c.p.
227	ml.	Ammonium Hydroxide, 28.42 per cent, Bakers, c.p.

Add distilled water to make 4.55 l. Filter and store in clean glass container.

Solution 2.

42.5	g.	Hydrazine Sulfate, Peacock Lab., Inc., Silver Spray Reducer
45.5	ml.	Ammonium Hydroxide, 28.42 per cent, Bakers, c.p.

Dissolve chemicals in distilled water and dilute to 4.55 l. Filter and store in clean glass container.

When ready to make mirrors:

Equal volumes of solutions 1 and 2 are applied by spray gun to the prepared glass on an almost vertical easel. An air pressure of about 40 lb. was used. The spray gun was supplied by the Peacock Laboratories, Inc., of Philadelphia, Pennsylvania.

Preparation of Specimens.

The glass regularly used in preparing test mirrors was single strength, Grade B American window glass. A limited number of specimens for special study were made with microscope slides and cover glasses. The window glass was cut to 6-in. squares for silvering.

The surfaces of the glass were cleaned with a paste of Spanish whiting and city water, applied by a cotton swab. The whiting was rinsed off with water and the entire surface swabbed with the sensitizing solution of stannous chloride. The stannous chloride sensitizer contains 0.5 g. stannous chloride (Peacock Lab., Inc., c.p.) per 1000 ml. of distilled water. An excess of the sensitizer is applied by use of a rubber sponge to the clean surface. It is then rubbed in evenly over the surface. Then, by means of a soft bristle brush, the sensitized surface is scrubbed with a good supply of distilled water. It is usually noticed that once the unwanted excess of stannous chloride is removed, the brush does not glide over the glass as easily as it did at the beginning. Finally, the surface is rinsed with the distilled water and the glass is then silvered without allowing the surface to dry even in spots, before application of the silvering solution. A few samples were made, omitting the use of the sensitizing solution.

For the silvering by evaporation, the glass surface was similarly cleaned, but after removing the whiting, the glass was rinsed with distilled water and acetone, and dried in a bell jar. Care was used to prevent contamination by dirt and grease.

Tests Performed.

Duplicate mirrors for different thicknesses were made by each process. Mirrors were classified as thin when they were fairly transparent and thick when about the weight of commercial mirrors or perhaps a little heavier. Electron diffraction studies were made on both surfaces of the silver coating; that is, the rear surface or the surface remote from the glass and the glass-silver interface, or the surface adjacent to the glass. For the diffraction studies, two or more specimens (8 × 4 mm.) were made from each square to afford multiple checks on observation.

Tests were made on the adhesion of the silver films to the glass by stripping with Scotch tape. A film completely removed from the glass by the tape was considered to have poor adhesion, one yielding spotty removal of the silver was classed as of fair adhesion, and mirrors were rated as having excellent adhesion if the silver film could not be affected by the Scotch tape.

The effect of aging was studied by placing the mirrors in a vacuum for four months in the presence of a dehydrating agent. Some specimens were heated in a vacuum to about 550° C. to note any changes that might be produced.

A number of mirrors were corroded with H_2S, NaOH, NCl, HNO_3, H_2SO_4, and NaKTa, and the surfaces and corrosion products were examined.

The influence of the sensitizing agent was studied in connection with the corroding agents and by the comparison of mirrors produced with and without the agent.

For the removal of the silver foil from the glass in order to study the glass-silver interface, several adhesives were tried. In general, no method gave satisfactory results since there was always a large number of failures. Three rather successful methods were used.

A drop of low melting point wax was allowed to fall on the back of the mirror and harden. A small piece of rectangular sheet metal (8 × 4 mm.) was then warmed sufficiently and pressed into the wax until there was left remaining a very thin layer of wax between the sheet of metal and the silver surface. The whole was allowed to cool and after trimming off the excess wax, the plate was lifted from the glass. In a number of cases the silver foil would adhere to the layer of wax and would expose the glass-silver interface. It often happened that the silver foil would become insulated by the layer of wax and would accordingly take on a charge in the diffraction camera and prevent taking a picture.

TABLE I.—*List of Interplanar Spacings d/n in Angstroms.*[a]

Rear Surface						Glass Silver Interface			Data from Literature					
Spray		Rochelle Epsom Salts		Weber		Spray	Weber	R. E. S.						
Thin Plate No. 22 b	Thick Plate No. 21 b	Thin Plate No. 39 a	Thick Plate No. 117 b	Thin Plate No. 36 b	Thick Plate No. 34 a	Scotch Tape Plate No. 18 b	Cu-Plated Plate No. 50 a	Cu-Plated Plate No. 48 b	Ag	SnO_2	SnO	Ag_2O	AgCl	NH_4Cl
d/n I	*d/n* I	*d/n* I	*d/n* I	*d/n* I	*d/n* I	*d/n* I	*d/n* I	*d/n* I	*d/n* I	*d/n* I	*d/n* I	*d/n* I	*d/n* I	*d/n* I
							3.79 w							3.85 m
										3.40 vs				
												3.35 vvw		
		3.19 m											3.20 m	
3.08 m				3.09 m	3.13 vw			2.91 m			2.97 s			
2.76 s		2.73 s										2.72 vs	2.77 s	2.72 s
2.68 m				2.69 s	2.67 vvw		2.67 vw	2.67 m		2.67 vs	2.66 m			
														2.22 w
2.36 s	2.34 s	2.42 w	2.37 m	2.39 w	2.35 m	2.41 w	2.38 vw	2.36 m	2.36 s	2.35 m	2.39 w	2.36 s		
2.04 s	2.01 s		2.03 m		2.03 w	2.13 w	2.01 vvw	2.06 w	2.04 s					
1.90 s		1.94 vs		1.92 vs									1.96 s	1.92 m
					1.82 vvw	1.84 vvw	1.87 w				1.89 w			
		1.78 vvw						1.77 m		1.77 vs	1.79 m			1.72 w
		1.65 w		1.65 m				1.64 vvw				1.67 m	1.67 m	
1.59 vvw		1.59 m		1.57 s			1.59 vvw				1.59 m		1.60 m	1.57 m
							1.53 w							
1.45 s	1.44 s	1.46 w	1.45 m	1.44 s	1.45 m	1.47 w	1.42 vvw	1.47 w	1.45 s	1.43 s	1.48 w	1.42 m		
		1.37 vw										1.36 w	1.38 w	1.37 w
		1.30 s								1.32 w	1.33 w		1.27 vw	1.29 vw

[a] Intensity of reflection indicated by: vs—very strong; s—strong; m—medium; w—weak; vw—very weak; vvw—very very weak

TABLE I.—*Continued.*

Rear Surface						Glass Silver Interface			Data from Literature					
Spray		Rochelle Epsom Salts		Weber		Spray	Weber	R. E. S.						
Thin Plate No. 22 b	Thick Plate No. 21 b	Thin Plate No. 39 a	Thick Plate No. 117 b	Thin Plate No. 36 b	Thick Plate No. 34 a	Scotch Tape Plate No. 18 b	Cu-Plated Plate No. 50 a	Cu-Plated Plate No. 48 b	Ag	SnO_2	SnO	Ag_2O	AgCl	NH_4Cl
d/*n* I	*d*/*n* I	*d*/*n* I	*d*/*n* I	*d*/*n* I	*d*/*n* I	*d*/*n* I	*d*/*n* I	*d*/*n* I	*d*/*n* I	*d*/*n* I	*d*/*n* I	*d*/*n* I	*d*/*n* I	*d*/*n* I
1.24 vs	1.22 vs	1.25 m	1.24 m	1.23 vs	1.26 m	1.26 m	1.31 w	1.25 m	1.23 s	1.21 m	1.22 w 1.19 w		1.24 m	1.22 w
1.18 vw	1.16 w	1.17 vvw 1.12 m		1.14 s	1.18 vvw		1.14 vw	1.15 vvw	1.18 w	1.16 w 1.10 w	1.17 w 1.07 w	1.18 vvw 1.08 vw	1.13 w	1.16 vw 1.11 vw
1.05 vvw	1.02 vvw	1.06 vvw 0.98 vvw		1.06 vw	1.09 vvw		0.98 vw	1.02 vvw	1.02 vw	1.05 vw	1.03 w	1.05 vw 0.96 vvw	1.06 vw 0.98 vw	1.03 w
0.93 m	0.93 s	0.93 m 0.92 m	0.93 w	0.94 s 0.92 s	0.93 w	0.93 vw		0.94 w	0.94 w 0.92 w			0.91 vvw	0.94 vw 0.92 w	0.92 vw
		0.87 vw		0.87 vvw									0.87 vw	0.87 vw
0.83 w	0.83 w	0.83 w	0.84 w	0.83 m	0.84 vw	0.83 vvw	0.84 vw	0.84 vvw	0.83 vw				0.84 vw	
0.78 w	0.78 w	0.79 vvw	0.78 vw	0.79 vvw 0.77 vvw	0.79 vw	0.79 vvw		0.80 vvw	0.79 w					
0.72 vvw	0.72 vvw	0.73 vvw		0.73 vw 0.72 vw	0.73 vvw		0.73 vvw	0.73 vvw						
0.69 m	0.69 m	0.69 vw	0.69 w	0.69 m 0.66 vvw	0.69 vvw	0.69 vw	0.64 vvw	0.69 vw	0.69 vw					
0.62 vvw	0.64 vvw	0.64 vvw 0.62 vvw	0.62 vvw	0.64 vvw 0.62 vvw	0.62 vvw									
		0.60 vvw		0.60 vvw										
0.56 vvw	0.56 w		0.57 vvw	0.56 w	0.56 vvw	0.57 vvw	0.56 vvw							
0.54 vvw	0.54 vw	0.54 vvw		0.54 w	0.53 vvw									
0.53 vvw	0.53 vw	0.53 vvw		0.53 w										
0.49 vvw	0.49 vvw	0.49 vvw		0.51 vvw		0.50 vvw								

Some silver coatings could very readily be removed with Scotch tape but the flexible specimens were not easily mounted in the camera.

The best results were obtained by electroplating the rear surfaces of the mirrors with copper of sufficient weight to permit the copper and silver to be stripped from the glass as a unit. These pieces were then trimmed to fit directly in the specimen holder of the electron camera and mounted for reflection. The copper plating baths did not appear to affect the silver films since the interface of several mirrors, stripped by means of Scotch tape, produced the same diffraction patterns as companion films stripped by means of the electroplated copper.

The following method for the electroplating was used:

Oxalto Plating Bath.

20	g.	Copper Sodium Oxalate Dihydrate
15	g.	Sodium Sulfate
20	g.	Boric Acid
1	l.	Distilled Water

Dissolve chemicals in the water, and use at 20 ma. per square inch. (This solution may be stored and used over again until it becomes exhausted.)

Acid Plating Bath.

200	g.	Copper Sulfate Pentahydrate
75	g.	Sulfuric Acid
1	l.	Distilled Water

Dissolve chemicals in the water, and use at 40 ma. per square inch. (This solution may be used repeatedly until it becomes exhausted.)

When ready to plate on silver films:

Plate mirrors for 10 min. using the Oxalto Bath, and follow with Acid Bath plating for 12 hr. or until copper deposit has desired thickness.

RESULTS AND DISCUSSION.

A total of 486 electron diffraction pictures were taken from various specimens by both reflection and transmission. In Table I are given d/n data from various representative pictures.

From the rear surfaces of thick mirrors very few patterns were obtained that were not at least fairly distinct.

The strength and sharpness of the rings were greatest for the Weber process, next for the spray process, and least for the Rochelle epsom salt.

Also, the number of rings present in addition to the silver pattern was greatest for the Weber process, next for the spray, and least or practically zero for the Rochelle epsom salt. There is accordingly a definite indication that the structures of the silver coatings differ and also that the amount of extraneous materials present is greatest for the Weber process and least for the Rochelle epsom salt process.

In the case of very thin mirrors prepared by all three processes, it was regularly observed that the patterns obtained by reflection from the back surfaces were strong and sharp as contrasted with the patterns from the back surfaces of thick mirrors. This result is somewhat surprising since it was observed that the thin mirrors appear to possess greater metallic luster than the thick ones. In his study, Sivertz (**4**) likewise observed that the back surfaces of thin mirrors have a higher reflectivity than the back surfaces of thick mirrors. The fact that a surface of higher metallic luster gives a more distinct electron diffraction pattern than a surface of lower metallic luster is contrary to the observation of Germer (**5**) who found that in general, surfaces inclined to be smooth and possessing metallic luster do not give good diffraction patterns.

For comparison, the d/n values taken from Hanawalt tables for Ag and the compounds AgCl, NH_4Cl, Ag_2O, SnO, SnO_2 are given in Table I. In no case was a perfect line-to-line agreement obtained for any of the compounds such as was obtained for silver. However, the amount of any compound present was relatively small so that fair agreement is all that could be expected. The specimens from mirrors made by any one of the processes varied greatly, indicating that the extraneous materials were randomly distributed over the mirrors. It was indeed difficult to get two specimens that would give the same patterns except that ordinarily there would always be a silver pattern predominating.

The various pictures obtained from the glass-silver interfaces also varied greatly even from the same mirrors. In a very large number of cases either no patterns at all or just one, two, or three broad bands were obtained. Both the absence of lines and the broad bands are characteristic of polished metal surfaces. In other cases some very fine diffraction patterns were obtained. It was not possible, however, to establish by electron diffraction any differences among the glass-silver interfaces for the three processes of mirror making.

In a few cases excellent silver patterns of the glass-silver interface were obtained that were most extraordinary. The patterns indicated either a change in the lattice of the silver or an error in the reading of the voltage. From the conditions under which the camera is operated, it is practically impossible to make an error of sufficient magnitude in reading the voltage to account for the change. On the other hand, it is hard to explain the change in the silver lattice from 4.06 to 3.80 Å. If there is a change in the lattice of the magnitude noted, it would mean that the density of the silver is about 15 per cent greater. It would be expected that the structure of the silver surface adjacent to the glass might be changed, but the normal silver structure with a changed lattice would ordinarily not be expected.

Specimens from each of the three processes stripped from glass by copper plating were mounted in a camera adjacent to heating grids, and

diffraction patterns were obtained by reflection from the glass-silver interface both before and after the grids were kept at a red heat (550° C.) for an hour. No changes in the patterns for any of the specimens were produced by the heat treatment.

Several pictures were made by reflection from the back surface of the silver and from the glass-silver interface for specimens when the sensitizing agent had been and had not been used. The patterns obtained when no sensitizing agent was used indicated the presence of silver alone.

A number of experiments were made in which the back surface of the silver on a mirror was treated with stannous chloride and a picture taken. No pattern at all was obtained. The surface was then washed with distilled water and faint rings were obtained. The surface was next washed with sodium hydroxide and a very satisfactory pattern of silver was obtained. This would indicate that the stannous chloride solution formed some kind of an amorphous layer over the surface.

In order to get an approximate idea as to how much of the stannous chloride remains on the glass surface after treatment, thin microscope-slide coverings were silvered and quantitative spectrum analyses were made of: (1) the glass not silvered; (2) the glass silvered but not sensitized; and (3) the glass silvered and sensitized.

The analyses showed a slight increase in the presence of tin when the sensitizer was used.

The suspected presence of a film between the silver and glass due to the sensitizing agent suggests that the optical constants of the interface might well be affected by the film. The validity of Drude's optical method in investigating transparent films on metals has been pointed out by Tronstad (6). Accordingly, observations by Drude's polarimetric method were made on the glass-silver interface of both sensitized and unsensitized mirrors. No difference for either the index of refraction or the reflecting power was found for the two surfaces.

Duplicate samples of all weights and types of silver mirrors were aged for four months by placing them in an exhausted vacuum-chamber in the presence of phosphoric acid anhydride. At the end of the period, visual inspection as well as an electron diffraction study, revealed no differences from freshly made mirrors. There was, however, a notable change in the adhesion of the spray process and the cold pouring process mirrors. These films, particularly the thick ones, were easily stripped from the glass by Scotch tape prior to placing in the vacuum. After vacuum aging, none of the mirrors made by any process, whether thick or thin, was affected by Scotch tape.

The spoilage occurs most frequently by the development of tiny white spots on the silver surface adjacent to the glass. The spots grow in size and often the silver film will start to peel from the glass. Quite frequently the back surface of the silver foil is free from any sign of spoilage,

even when the glass-silver interface presents a decided spoilage appearance. There is thus a preferential spoilage effect, that takes place on the silver surface adjacent to the glass. This rather suggests the occurrence of some material between the glass and the silver, that accelerates the spoilage.

An effort was made to determine the nature of the spoilage process by making electron diffraction patterns of the glass-silver interface from spoiled mirrors. Several old mirror specimens supplied by the Hobbs Glass Limited were used in part in this test. As the specimens were taken from mirrors that showed increased spoilage both the number and sharpness of the lines generally increased. In one case where the mirrors had turned completely white and the silver was peeling from the glass, nice diffraction patterns of silver were obtained without the presence of any extra lines due to other materials. X-ray patterns made from the whitish silver scraped from the glass showed nothing but silver.

The failure to detect any chemical compounds associated with the spoilage of mirrors suggested the use of certain corroding agents and a study of the resulting compounds. A few mirrors were exposed to hydrogen sulfide gas. Electron diffraction patterns by reflection did not indicate the presence of any silver sulfide until the mirrors had been rather extensively corroded. Even though the corrosion effect on a surface was readily visible, the diffraction pattern consisted only of that of silver. However, when the surfaces became quite blackened and heavily corroded, there was present, along with the silver pattern, lines of silver sulfide.

Treatment with hot sodium hydroxide solution lifted the silver films from the glass. Even the thinnest films were loosened intact. The electron diffraction patterns by transmission showed the presence of silver only. The same result was obtained when a solution of the basic salt, sodium potassium tartrate, was used as the corroding agent.

Mirrors were corroded by means of hydrochloric acid until there was left on the glass nothing but a white powder. The X-ray diffraction pictures of the residues showed a rather strong pattern of silver and peculiarly enough nothing for silver chloride but a very excellent agreement for ammonium chloride. This would rather indicate the presence of some ammonium compounds on the silver which upon treatment with hydrochloric acid gave ammonium chloride. X-ray and electron diffraction pictures made of mirrors corroded by nitric and sulfuric acid showed the presence of many lines in addition to those of the silver pattern. The lines could not be identified as belonging to any known compounds.

During the corrosion by acids there was noted a marked tendency for the corrosion to take place preferentially at the glass-silver interface. White spoilage occurred and the mirror as such was destroyed before

there was any appreciable effect on the rear surface, where the acids were applied.

The preferential spoilage process that was found so frequently to take place on the glass-silver interface suggested that the phenomenon may be due to the hygroscopicity of the sensitizing layer between the silver and the glass. A number of spray mirrors were placed under a bell jar in the presence of water. At first, the usual white spots developed and subsequently almost the whole of the mirror surfaces turned white. Also, the silver foil became more easily removable from the glass. In some cases it even peeled from the glass of its own accord. The presence of water apparently has a decided influence on the adhesion. Evaporated mirrors placed under the bell jar with the other mirrors showed no spoilage. However, in the case of very thin chemically deposited mirrors there was little tendency to show spoilage but the silver foil was found to have less adherence to the glass. The whitish nature would not be expected to be so pronounced due to the transparency of the silver film.

A marked difference between chemical and evaporated mirrors is the presence of foreign materials in the chemical mirrors. It, therefore, seems logical that the foreign materials may act as spoiling agents. The foreign materials, however, seem to occur in greater quantities on the backs of thin mirrors than on thick mirrors, and spoilage and poor adhesion is more prevalent in thick mirrors than in thin ones. The explanation of this may be that spoilage is a mechanical rather than a chemical process in the cases involved. The impurities imbedded in a layer adjacent to glass absorb moisture or suffer some mechanical change that causes a frosted appearance of a very thin layer adjacent to the glass. In thick mirrors this frosted layer is thick and is plainly visible. In thin mirrors the layer is not so thick and the mutilation is not so pronounced.

SUMMARY AND CONCLUSIONS.

A. Back Surface of Mirrors.

1. The back surfaces of silver mirrors deposited by chemical reduction by all three of the processes described are predominately crystalline silver with the presence of considerable quantities of various chemical compounds. The compounds ranging in amount from zero to about 10 per cent of the surface layer, varied from mirror to mirror and from place to place on the same mirror.

2. AgCl and NH_4Cl in varying amounts were found both together and separately on the rear surfaces of thin mirrors made by all three processes.

3. On Rochelle epsom salts thick mirrors, silver alone was usually found.

4. On thick mirrors made by the spray method there were frequently

present extra materials, but never in sufficient amounts to permit identification.

5. On Weber thick mirrors, considerable foreign materials were present. SnO_2, AgCl, or NH_4Cl were sometimes among them.

B. Glass-silver Interface.

1. The silver surface adjacent to the glass presented a crystalline nature in some cases and in other cases the nature of an amorphous or polished surface. The surface varied from mirror to mirror and from spot to spot in the same mirror.

2. There were present extra materials in all three types of mirrors, but not in sufficient quantities to make identification possible. However, in the case of Weber mirrors there was good indication of the presence of SnO.

3. The amorphous behavior may be due to one of three types of surface:

(*a*) The silver surface may take a truly amorphous structure due to the deposition on the amorphous surface of glass.

(*b*) The surface may behave as an amorphous one due to the smoothness produced by deposition of the silver on the smooth glass surface.

(*c*) The sensitizing solution of stannous chloride may produce an amorphous layer of stannic oxide or some other compound.

C. Adhesion.

1. The adhesion of freshly made mirror films is classed as follows:

Poor—Heavy and medium spray process mirrors
Fair—Thin spray process mirrors
Heavy Weber cold pouring process mirrors
Excellent—Very thin spray process mirrors
Medium and thin Weber cold pouring process mirrors
All R.E.S. hot table process mirrors

2. The adhesion was greatly improved in the case of all spray and thick Weber processed mirrors by aging for four months in a vacuum in the presence of a strong dehydrating agent. There were no other detectable changes produced in the mirrors. It is believed that the improvement was due to drying and that there were no accompanying changes in structure or chemical composition.

D. Spoilage.

1. No evidence was found that ordinary spoilage is a chemical reaction.

2. The deterioration of mirrors is greatly accelerated by moisture.

3. Spoilage in the presence of moisture is either a mechanical or chemical process resulting from impurities imbedded between the silver and glass.

ACKNOWLEDGMENT.

This work was done under contract for the Hobbs Glass Limited of London, Ontario, Canada. The authors wish to express their appreciation to the Company for its cooperation and financial support. They also want to thank K. P. Gladney, formerly of that company, for his advice and continued interest in the work.

REFERENCES.

(1) V. KOHLSHUTTER AND E. FISHCHMANN, "Über das Spiegelsilber," *Liebig's Annals*, Leipzig, Vol. 387, p. 88 (1912).

(2) P. v. SCHERRER, "The Determination of the Internal Structure and the Size of Colloidal Particles by Means of X-Rays," in R. ZSIGMONDY, "Kolloidchemie," Third edition, Leipzig, Otto Spamer, p. 387 (1920).

(3) VON H. VON WARTENBERG, "Über die Beschleunigung der Glasversilberung mit Zinnchlorür," *Z. anorg. Chem.*, Vol. 190, p. 185 (1930).

(4) C. SIVERTZ, private communication.

(5) L. H. GERMER, "Diffraction of Electrons by Metal Surfaces," *Phys. Rev.*, Vol. 43, p. 724 (1933).

(6) LEIF TRONSTAD, "The Validity of Drude's Optical Method of Investigating Transparent Films of Metals," *Transactions of the Faraday Society*, Vol. XXXI, September, 1935, pp. 1151–1158.

ELECTRON LENSES OF HYPERBOLIC FIELD STRUCTURE.*

BY

REINHOLD RÜDENBERG.[1]

Part II.

SUMMARY.

Increasing lens voltage, higher than the incident electron voltage, at first blocks the beam and then converts the electron lens into a curved mirror, the focal properties of which are analyzed.

The embodiment of hyperbolic lenses is discussed by means of the boundary conditions which may be rigorously or approximately satisfied in actual designs. The effects of lateral apertures and windows on the imaging qualities of the field are considered in detail.

Expressions are derived for velocity-, angular- and aperture-defects, the latter being merely a surface effect of the hyperbolic field. They all depend on a few parameters only of the lens field and are relatively small in magnitude. An experimental verification of the field structure with partial compensation of the defects shows favorable imaging qualities.

Two-dimensional fields, constituting electron cylinder lenses, are considered in a similar way, leading to analogous formulations for the cardinal properties.

7. CURVED MIRROR EFFECT.

For an electrostatic field of such power that it exceeds the blocking condition of Eq. 46 the transmission constant B is imaginary, and the term of Eq. 31 with the constant C becomes controlling. By effect of the double-valued cosh-function, this term represents a mirror action in the z-direction (8).[2] In the r-direction, the oscillation of Eq. 30 holds true also in this case.

By elimination of the time t from Eqs. 30 and 31 and use of Eq. 32, the trajectories are

$$\frac{z}{C} = \cosh\left[\sqrt{2}\left(\cos^{-1}\left(\frac{r}{A}\right) - \varphi\right)\right];$$

or (83)

$$\frac{r}{A} = \cos\left[\frac{1}{\sqrt{2}}\cosh^{-1}\left(\frac{z}{C}\right) + \varphi\right].$$

Figure 22 shows the development in space of these electron paths, each defined by a certain value of the phase angle φ. All the trajectories penetrate the field up to an abscissa $z/C = 1$ and then return on another

* Paper read at the Philadelphia meeting of the Electron Microscope Society of America on December 11, 1947; Part I appeared in the October, 1948, issue of this JOURNAL, p. 311.

[1] Gordon McKay Professor of Electrical Engineering, Graduate School of Engineering, Harvard University, Cambridge, Mass.

[2] The boldface numbers in parentheses refer to the references appended to this paper.

branch of the cosh-function. Thus, the plane $z = C$ represents a mirror surface at which the individual rays are reflected, their incidence and emergence, however, being tangential to this surface. The actual reflecting action is produced in the volume of the field, quite differently from the abrupt reflection of light at a surface. The individual ray for $\varphi = 0$ returns exactly on the incident path. All the other rays are incident on one side and reflected on the other side of this $\varphi = 0$ path.

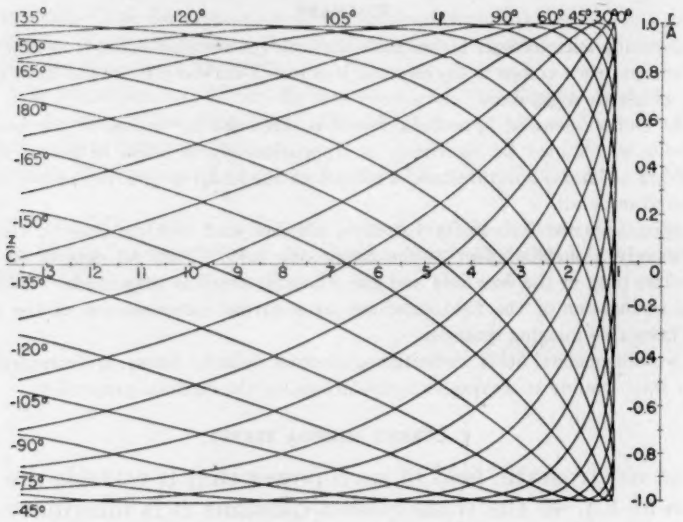

FIG. 22. Electron trajectories in hyperbolic mirror field.

The velocity of the electrons in the radial direction is given again by Eq. 38. In the axial direction, however, the velocity is

$$v_z = \frac{dz}{dt} = \mu C \sinh \mu t. \tag{84}$$

Eliminating t by Eq. 31 yields

$$\frac{v_z}{\mu C} = \sinh\left(\cosh^{-1}\left(\frac{z}{C}\right)\right) = \pm\sqrt{\left(\frac{z}{C}\right)^2 - 1}. \tag{85}$$

Figure 23 shows that the axial velocity again follows a hyperbola, only that compared with Fig. 9 the axes are turned by 90°. Hence, the axial velocity of any incident electron becomes zero and reverses its sign at the plane $z = C$, where merely radial velocity remains. Only for the trajectory $\varphi = 0$ do both axial and radial velocities vanish at the point of reflection, as seen from Fig. 22.

An electron entering the field at the plane $z = -Z$ with axial velocity V proceeds with velocity v_z according to Eq. 85, as shown by

Fig. 23. This gives the boundary condition

$$V = \pm \mu \sqrt{Z^2 - C^2}. \tag{86}$$

Using Eqs. 31 and 41 for μ and V gives

$$E_V = p(Z^2 - C^2). \tag{87}$$

Hence the reflection constant of the mirror is

$$C = \sqrt{Z^2 - \frac{E_V}{p}} = \sqrt{Z^2 - \left(\frac{V}{\mu}\right)^2}, \tag{88}$$

which is in contrast to Eq. 44 for the transmission constant of a lens.

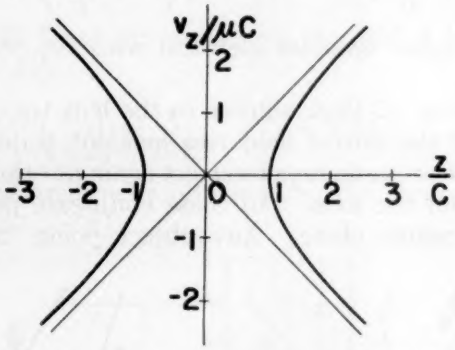

FIG. 23. Velocity distribution in mirror field.

Expressed by the parameters of the hyperbolic field, as shown in Fig. 5, the reflection constant becomes, with use of Eq. 26,

$$C = \sqrt{Z^2 - \frac{E_V}{E}\left(Z^2 + \frac{R^2}{2}\right)} = \sqrt{\left(1 - \frac{E_V}{E}\right) Z^2 - \frac{1}{2}\frac{E_V}{E} R^2}. \tag{89}$$

This again depends merely on three parameters, the half-thickness Z, the aperture-radius R and the voltage-ratio E/E_V which always must be larger than unity.

Since the electrons never can reach the center plane, it is not necessary to build up the complete field structure as is done in Fig. 5. In many cases it will be sufficient to limit the mirror on the rear side by an equipotential cone, as shown by Fig. 24(a). In this case the radius of the annular hyperboloid is $R = 0$, and the reflection constant thus will be

$$C = Z\sqrt{1 - \frac{E_V}{E}}. \tag{90}$$

It even might be sufficient to provide merely for one of the inner lateral hyperboloids, as shown by Fig. 24(b), with its vertex at a distance Z_1 from the center, which of course must be smaller than the distance C of the reflecting surface. In this case there is no annular

hyperboloid, and therefore the difference of potential between two lateral hyperboloids determines the voltage E here applied. Thus, with use of Eq. 12 we have for $r = 0$

$$E = \Phi - \Phi_1 = p(Z^2 - Z_1^2) \tag{91}$$

and the power of the field is

$$p = \frac{E}{Z^2 - Z_1^2}. \tag{92}$$

The reflection constant of the unilateral mirror field is now by Eq. 88

$$C = \sqrt{Z^2 - \frac{E_V}{E}(Z^2 - Z_1^2)} = \sqrt{\left(1 - \frac{E_V}{E}\right) Z^2 + \frac{E_V}{E} Z_1^2}. \tag{93}$$

For $Z_1 = 0$ this value becomes identical with Eq. 90 when using the asymptotic cone.

We see from Fig. 22 that, similar to the lens trajectories of Fig. 6, at every point of the mirror field two incident trajectories are intersecting and that these same rays intersect again at other abscissas at the same distance from the axis. All these conjugate points are here on one side of the center plane. Any object point, therefore, appears

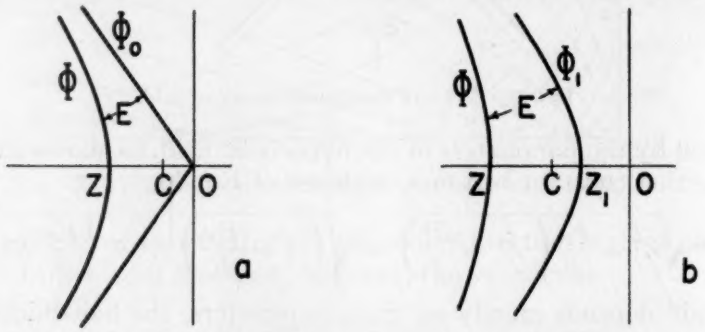

FIG. 24. Equipotential boundaries for electron mirror, (*a*) with rear cone, (*b*) with rear hyperboloid.

imaged by the reflecting electron rays at consecutive image points, all having a magnification ± 1. If the incident electron beam is uniform over the cross section, the image formation of the electrostatic mirror is free of aberration within the entire volume of the field.

The cardinal points of a reflecting field which is limited by a plane radial boundary can be derived in a corresponding way as formerly used for lens fields. The condition of entrance of a parallel beam at $z = Z$, as in Fig. 25, is $r/A = 1$. Thus, from Eq. 83 we have for determination of the phase angle

$$\frac{Z}{C} = \cosh\left[\sqrt{2}(0 - \varphi)\right]; \qquad \varphi = \frac{1}{\sqrt{2}} \cosh^{-1}\left(\frac{Z}{C}\right). \tag{94}$$

These rays, therefore, follow trajectories within the mirror field, as given by

$$\frac{r}{A} = \cos\left[\frac{1}{\sqrt{2}}\cosh^{-1}\left(\frac{z}{C}\right) + \frac{1}{\sqrt{2}}\cosh^{-1}\left(\frac{Z}{C}\right)\right]. \tag{95}$$

After reflection the electron paths are recessive and leave the lens field at the same boundary, $z = Z$, as indicated in Fig. 25. The exit radius, therefore, is given by

$$\frac{r}{A} = \cos\left[\sqrt{2}\cosh^{-1}\left(\frac{Z}{C}\right)\right]. \tag{96}$$

From there on the electron path is rectilinear, intersecting the axis at the focal point.

The focus will be at the surface of the field if in Eq. 96 $r/A = 0$, giving the condition

$$\cosh^{-1}\left(\frac{Z}{C}\right) = \frac{\pi}{2\sqrt{2}}; \qquad \frac{Z}{C} = 1.68; \qquad \varphi = \frac{\pi}{4}. \tag{97}$$

Herein the phase angle φ is obtained by the second Eq. 94. Hence,

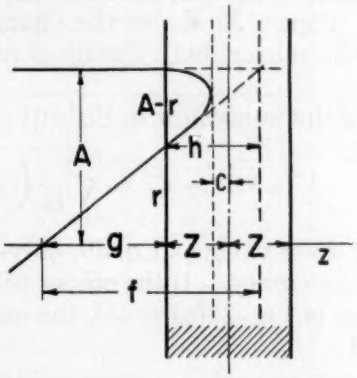

FIG. 25. Parallel incident ray and cardinal mirror points.

the focus lies outside the mirror field only if the width of the field is smaller than 45°. This can be graphically verified by means of Fig. 22.

The slope of the rays is given by the derivative, the expression for which by Eq. 83 is generally

$$\frac{dr}{dz} = -\frac{A}{C}\frac{\sin\left[\frac{1}{\sqrt{2}}\cosh^{-1}\left(\frac{z}{C}\right) + \varphi\right]}{\sqrt{2\left(\left(\frac{z}{C}\right)^2 - 1\right)}}. \tag{98}$$

This is different in both numerator and denominator from the corresponding slope in the lens field, see Eq. 55. At $z = C$ the denominator is zero determining the position of the reflecting plane.

For rays of parallel incidence, insertion of the phase angle φ from Eq. 94 gives the slope of the emerging ray at the abscissa Z

$$\frac{dr}{dz} = -\frac{A}{C}\frac{\sin\left[\sqrt{2}\cosh^{-1}\left(\frac{Z}{C}\right)\right]}{\sqrt{2\left(\left(\frac{Z}{C}\right)^2 - 1\right)}}. \tag{99}$$

The back-focus of the mirror field as seen by Fig. 25 is

$$g = \frac{r}{dr/dz} \tag{100}$$

applied to the exit point of the ray. With use of Eqs. 96 and 99 we obtain,

$$g = \frac{\sqrt{2}C\sqrt{\left(\frac{Z}{C}\right)^2 - 1}}{\tan\left[\sqrt{2}\cosh^{-1}\left(\frac{Z}{C}\right)\right]}. \tag{101}$$

This value is independent of the amplitude A, indicating freedom from any aperture defect. Figure 26 shows the change of the back-focus with half-width Z of the mirror, both distances plotted as ratio to the reflection constant C.

The main factors of the numerator in Eq. 101 are with use of Eq. 89

$$C\sqrt{\left(\frac{Z}{C}\right)^2 - 1} = \sqrt{Z^2 - C^2} = \sqrt{\frac{E_V}{E}\left(Z^2 + \frac{R^2}{2}\right)}. \tag{102}$$

Formally, this has the same value as Eq. 59, only that here the voltage ratio E_V/E is smaller than unity. If the mirror field is provided only on the side of incidence, as in Fig. 24(a) or (b), the main factors of Eq. 101 are with use of Eq. 93

$$C\sqrt{\left(\frac{Z}{C}\right)^2 - 1} = \sqrt{\frac{E_V}{E}(Z^2 - Z_1^2)}. \tag{103}$$

This gives for the same voltage across the electrodes a smaller back-focus g due to the higher power of the field.

The emerging rays reflected from a parallel incident beam, as in Fig. 25, seem to come from a depth h beyond the surface, defining the position of the principal reflecting plane of the mirror. This depth is determined by radius and derivative at the exit point as

$$h = \frac{A - r}{dr/dz} = \sqrt{2}C\sqrt{\left(\frac{Z}{C}\right)^2 - 1}\cdot\tan\left[\frac{1}{\sqrt{2}}\cosh^{-1}\left(\frac{Z}{C}\right)\right]. \tag{104}$$

Herein Eqs. 96 and 99 are used, and the cosine and sine functions are combined into the tangent of half the argument. Figure 26 shows the

change of this value with increasing width of the field. Where h is larger than Z, the principal plane is on the rear side of the field center.

The focal length of the electron mirror, according to Fig. 25, is

$$f = \frac{A}{dr/dz} = \frac{\sqrt{2}C\sqrt{\left(\frac{Z}{C}\right)^2 - 1}}{\sin\left[\sqrt{2}\cosh^{-1}\left(\frac{Z}{C}\right)\right]}. \tag{105}$$

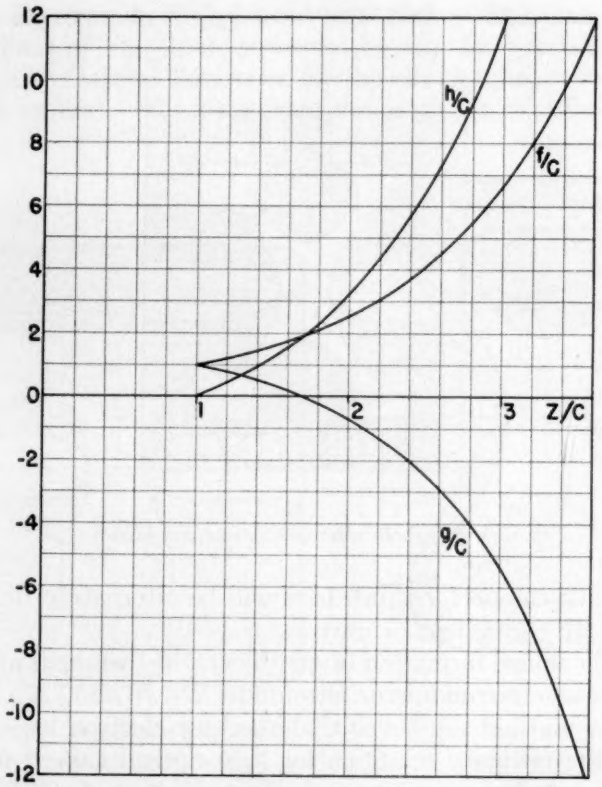

FIG. 26. Change of cardinal values with mirror thickness.

Its value as ratio to C is also plotted in Fig. 26.

When discussing these curves it should be noted that the abscissa, by Eq. 89, is

$$\frac{Z}{C} = \frac{1}{\sqrt{1 - \frac{E_V}{E}\left[1 + \frac{1}{2}\left(\frac{R}{Z}\right)^2\right]}}. \tag{106}$$

Thus, for values of E/E_V and Z/R which are near to the limiting condition (46), Z/C attains great magnitude. With higher voltage and

greater depth, however, Z/C decreases gradually towards unity. Electron mirrors of moderate value of Z/C, therefore, require considerable voltage E and small radius R with respect to Z.

In the range shown in Fig. 26, f is positive throughout and the focus lies before the principal plane. Thus, the field effect is converging, like that of a concave mirror in light-optics. For $Z/C = 4.66$, however, the sine in Eq. 105 changes sign. Hereby f becomes negative and a diverging electron mirror is formed, the properties of which are similar to those of a convex mirror in light optics. In the interval between $Z/C = 4.66$ and $Z/B = 4.55$, the focal length changes its sign many

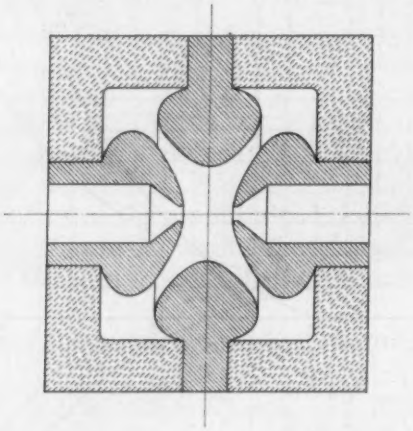

FIG. 27. Hyperbolic electrostatic lens, mushroom type.

times and thus the performance here will be alternately that of a converging and diverging lens or mirror.

If used for image formation of an object, the distances and the magnification for an electron mirror also follow Eq. 70 and 72. This can be derived by a method similar to that used for electron lenses and coincides with the ordinary relations for light-optical curved mirrors. In the electron case, however, the performance is that of a "thick" mirror.

If we consider a wide range of velocities of the incident electron beam, to cover both solutions of Eq. 31 which are separated by the blocking condition (46), we realize that a hyperbolic electron lens will act as a high-pass filter, and a hyperbolic electron mirror as a low-pass filter. They may be utilized singly or in combination for the purpose of selection of velocities.

8. BOUNDARIES OF THE FIELD.

There are several ways of arranging for the embodiment of an electron lens which insure the production of a hyperbolic field structure.

One method consists in building up some of the equipotential surfaces by conducting areas. Such hyperboloids may serve as electrodes or poles of the electron lens. If they are extended wide enough along the asymptotic cones in Fig. 2, they will secure the formation of the correct field structure in the interior space.

Figure 27 shows a mechanical setup of such a lens. The two lateral electrodes are at the same potential, and the intermediate annular electrode is charged to a different potential. The three electrodes may be kept in position by two insulating angular rings. The surfaces of the electrodes are shaped hyperboloidally according to any of the equipotential lines of Fig. 2, as expressed by Eq. 18. Axial apertures are provided in the lateral electrodes for the electron beam to enter and to leave the lens field. Far away from the beam the hyperboloidal bound-

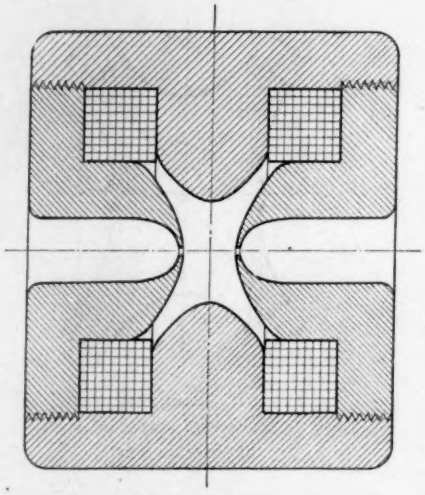

FIG. 28. Hyperbolic magnetic electron lens.

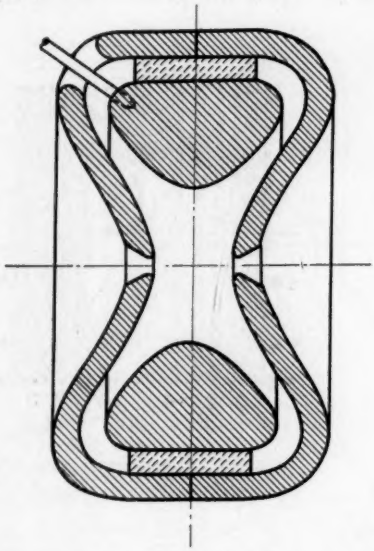

FIG. 29. Hyperbolic electrostatic lens, plate type.

aries of the active lens space are curved into softly rounded shapes of the electrodes in order that these will stand high voltage.

A design of a magnetic hyperbolic lens is shown in Fig. 28. Two coaxial, current-carrying coils surround the lateral pole pieces exciting them in one polarity, which is opposite to the polarity of the intermediate annular pole. The inner surfaces of the magnetic circuit are shaped according to any of the hyperbolic lines shown in Fig. 2, except for an aperture in each of the lateral pole pieces. If the pole faces are made of highly permeable magnetic steel, the field in the interspace will have the structure of Eqs. 12 and 14. Instead of exciting such lens by electric current a permanent magnetization of the magnetic circuit may be used.

Another setup of an electrostatic hyperbolic lens is shown in Fig. 29. Here the lateral electrodes are formed as curved plates, joined together and fixed to the annular electrode by means of an insulating ring.

Another method of securing the distribution of a hyperbolic field is shown in Fig. 30. A number of concentric rings are arranged around the axis, each ring being charged to a potential given by Eq. 12 for the position z and r of the individual conducting ring. In Fig. 30 the necessary potentials of the various rings are indicated by the numbers, for a certain example.

Figure 31 shows a combination of equipotential surfaces and heteropotential rings, the latter arranged for correct termination of the field near the asymptotes. For each ring the potential, again, is determined by its radius r and its axial distance z, according to Eq. 12, and thus it is between the potentials of the main electrodes. By means of such

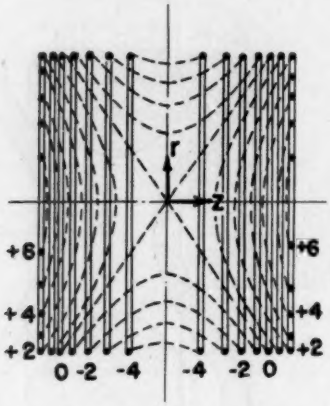

FIG. 30. Electrostatic ring lens of hyperbolic potential.

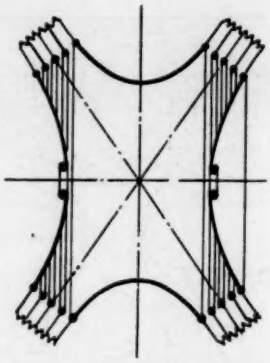

FIG. 31. Combined equipotential and ring hyperbolic lens.

intermediate rings the extension of the conducting surfaces along the asymptotes can be greatly reduced without detrimental reaction on the field structure near the beam. Therefore, in comparison to Fig. 27 there will remain a wider gap between the hyperboloidal electrodes, which is advantageous for the use of high lens voltage.

A third method of producing a rigorous hyperbolic structure is shown in Fig. 32 by an example in which the field between the electrodes is terminated by the use of semi-conducting sheets. These are fixed here on the inner surface of two insulating rings, which may be used also for keeping the main electrodes at the proper distance. The voltage drop along the resistance coating can be adjusted so that the potential follows Eq. 12 along the sheet. Since the equipotential lines near the asymptotes of the field structure are nearly equidistant, a uniformly-conducting, high-resistance sheet may be used with good

approximation. Any distorting influence on the field structure by the finite ends of the actual electrodes thus will be excluded. In consequence the gap between the electrodes can be kept wide, thereby increasing the high-voltage security of the lens.

Another example of a hyperbolic field structure, terminated by the means already described, is shown in Fig. 33. In this case the field section used lies entirely at one side of the origin and thus the two lateral equipotential hyperboloids are curved in the same direction. The field between these electrodes acts purely accelerating on the electron beam which may be produced by a photo-cathode on the left-hand side of this image converter. A cylindrical surface around the beam is formed by a co-axial insulating tube, coated with a semi-conducting layer. The resistance of this sheet varies in z direction so that the potential distribution along the surface will follow a quadratic law as

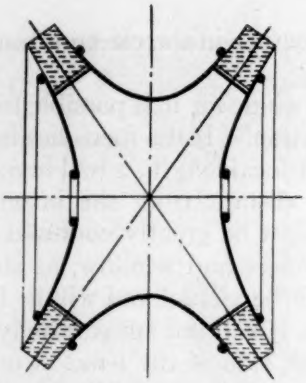

FIG. 32. Combined equipotential and semiconductor hyperbolic lens.

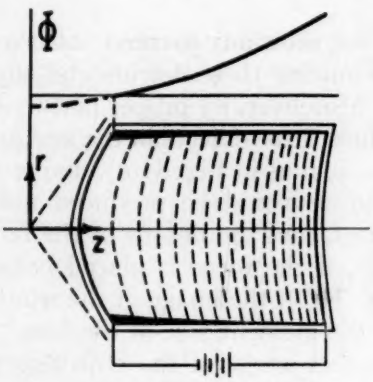

FIG. 33. Hyperbolic accelerating image converter.

prescribed by Eq. 12. For this purpose the unit resistance should be essentially proportional to the distance z. As indicated in Fig. 33, this can be secured by a decreasing thickness of the resistance coating with increasing z.

In all those cases where an external electron beam enters or leaves the lens through the boundaries of the field, apertures must be provided in the centers of the lateral electrodes. An ideal way of arranging such an aperture for the electron beam, without causing any perturbation of the field structure, is the application of a window consisting of a thin conducting foil through which the electrons can pass. The foil may be coated for rigidity on a permeable material of low density. Arranged with very slight curvature as needed for the surfaces near the axis, such foils can be made of sufficient conductivity to act equipotentially and thus to secure the correct structure of the electrostatic field. Such a foil, to be sure, would show certain effects due to absorption and scattering of electrons in the beam. However, some metals exist which

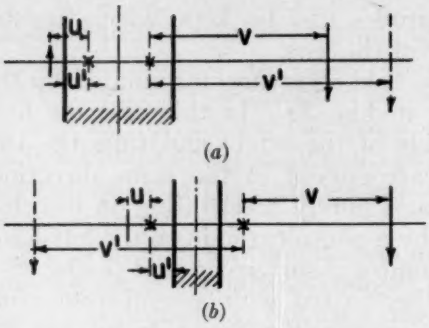

FIG. 34. Effect of lens windows on quality of image.

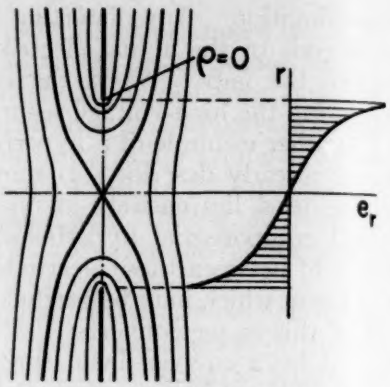

FIG. 35. Field structure in thin plate aperture.

do not show any marked pattern of structure in the electron beam, thus minimizing these detrimental effects.

Moreover, by proper placing of the windows, it is possible further to reduce these defects in the image formation. If the focus lies inside the lens field as in Fig. 34(*a*), due to a short focal length, a real image of the window would be produced not very distant from the image of the object, and the details of the latter might be greatly confused. However, if the focus is placed between object and window, as shown by Fig. 34(*b*), the image of the window will be virtual and will lie far away on the incident side of the lens. Thus, it will not substantially disturb the real image of the object on the exit side of the lens. Under such circumstances, even a granular window might give a diffuse background of the principal image, but no perturbation of its pattern.

If subsequent lenses are used, forming a compound instrument, the same viewpoints will hold for all of the front windows and for the inter-

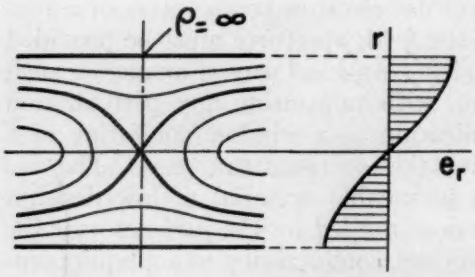

FIG. 36. Field structure in cylindrical aperture.

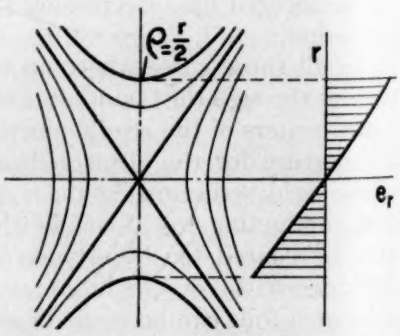

FIG. 37. Field structure in hyperboloidal aperture.

mediate images near the second or third electron lens. The rear windows will in all circumstances produce merely a diffuse background.

The conventional way of passing an external electron beam through the lens is the arrangement of openings in the centers of the lateral electrodes. It is well known, however, that such apertures produce additional lens fields of their own. Hence, they will give rise not only to supplementary focusing effects, but also to aberrations of the rays, due to the imperfect structure of their aperture field.

A proportional change of the radial field strength should be expected if the rim of the aperture were shaped between the two opposite extremes of Figs. 35 and 36 which have first been investigated by Ollendorff (3) and Gray (4). We know that a hyperbolic field, as shown in comparison by Fig. 37, will satisfy this condition. A rigorous application of the hyperbolic field structure to provide apertures in the

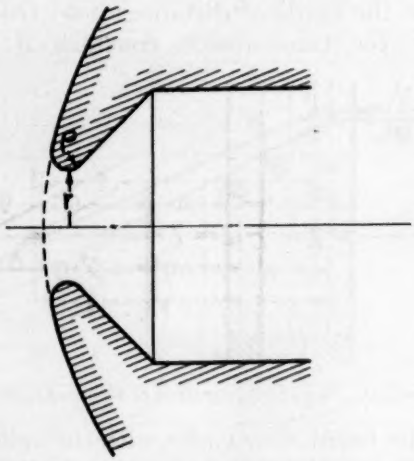

FIG. 38. Rounding off of lateral lens apertures.

lateral electrodes is not feasible. However, we realize by comparison of Figs. 35, 36, and 37 that the essential radial field strength will be widely linearized if we use the main geometric characteristic of a hyperbolic opening, namely its radius of curvature at the rim.

Hence, if rounding off the lateral apertures by a radius in the meridian plane of half the value of the aperture radius in the radial plane, as indicated by Eq. 20, we will approximate a hyperbolic field structure within the aperture. Thereby we should avoid the formation of excessive field distortions and beam aberrations, as produced by the limiting cases of Figs. 35 and 36. Figure 38 shows the shape of a properly rounded off aperture in detail.

We have seen from the foregoing discussion that a uniform parallel electron beam incident on a hyperbolic field structure will not experience any aberration in connection with the transmission within the

formative space of the field. However, at the entrance and exit of the field space it seems not to be possible to eliminate such perturbations entirely, but only to minimize them to a considerable degree. Hence, while volume aberrations of uniform beams are avoided in electron lenses as here described, surface aberrations remain which will be studied in greater detail. Further defects will be experienced if the beam entering the lens field is non-uniform in the velocity of its rays, either in magnitude or in the direction with respect to the lens axis.

9. VELOCITY ABERRATION.

If the incident beam is parallel but not homogeneous as supposed heretofore, containing electrons of a variety of speeds, there develops a velocity aberration of the rays throughout the entire structure of the hyperbolic field. Sometimes such a type of defect is designated as "chromatic aberration" in analogy to the light-optical phenomenon.

Our formulas for the cardinal distances hold true for any incident velocity. However, the transmission constant B, instead of being

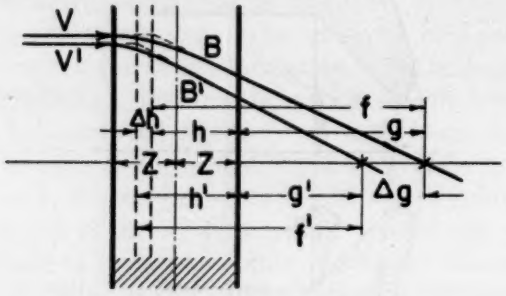

FIG. 39. Velocity aberration of electron rays.

constant for the entire beam, now varies with the velocity voltage of the individual electron rays. We will derive the displacement of the focus with varying velocity and the corresponding change in focal length, as indicated in Fig. 39.

For a lens of a given half-length Z we divide Eqs. 58 and 62 for the focal position and the focal length by Z and consider B/Z as the independent variable, which is directly determined by the incident velocity voltage E_V (see Eq. 49). In order to derive a simple interrelation, we substitute the right-hand side of Eq. 46 into Eq. 49 after denoting the blocking velocity voltage of Eq. 46 by E_{V0}. Thus we obtain the ratio of incident electron velocity voltage to incident blocking voltage

$$\frac{E_V}{E_{V0}} = 1 + \left(\frac{B}{Z}\right)^2. \tag{107}$$

From Figs. 15 and 17 there are plotted in Fig. 40 the ratios f/Z for the focal length and g/Z for the back-focus *versus* the ratio E_V/E_{V0} just mentioned. These curves show clearly the influence of the incident

electron voltage E_V on the focal values while all other magnitudes are kept constant. In order to relate the incident electron voltage directly to the lens voltage E, rather than to the blocking velocity voltage, we derive from Eq. 46

$$\frac{E_V}{E} = \frac{E_V/E_{VO}}{1 + \frac{1}{2}\left(\frac{R}{Z}\right)^2}. \tag{108}$$

Thus, for different aperture ratios R/Z of the lens, the scales for E_V/E under the abscissa of Fig. 40 can be plotted. There is added a scale for Z/B corresponding to Eq. 107, all these abscissa scales being convenient for various purposes.

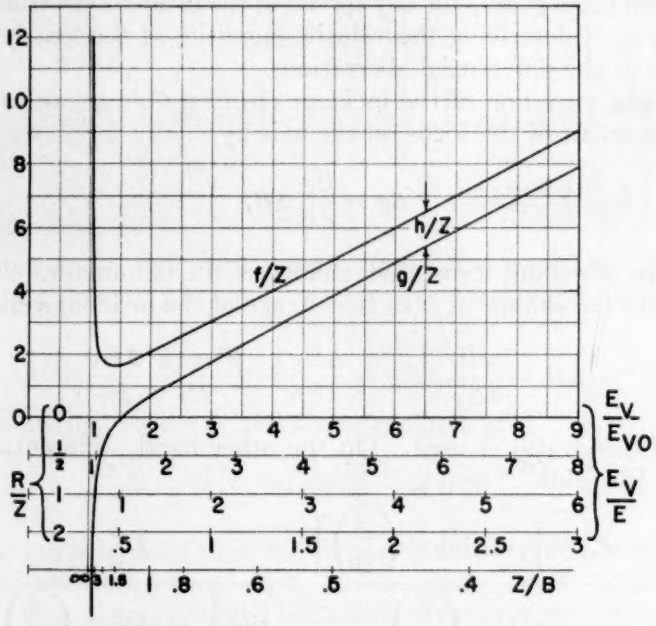

FIG. 40. Change of cardinal values with ray velocity.

For an incident electron voltage just equal to the blocking electron voltage, both focal length and back-focus are indeterminate. For rising electron voltage the back-focus g after initial oscillations increases steadily from negative values through zero to high positive values. The focal length f, however, decreases at first, reaches a minimum, and then increases, always remaining larger than the back-focus by the value h, the distance of the principal plane. The minimum of f/Z occurs at $E_V/E_{VO} = 1.44$, which corresponds to $Z/B = 1.5$ as seen from the scale at the bottom of Fig. 40. For this value, or for the corresponding values of E_V/E taken from the intermediate scales, the focal

length is independent of small variations in the incident electron velocity.

However, the actual position of the focus, as given by the back-focus g, is for the most part of greater significance than f, as seen by discussion of Eqs. 70 and 72 for distance and magnification of the image. Hence, Fig. 40 shows that a truly akinetic or "achromatic" lens actually does not exist. However, in a certain range where f varies slightly and g varies not too much, the lens will have relatively favorable velocity qualities. On the other hand, for any given focal length or given magnification, the curves of Fig. 40 may be used to derive a lens of least total velocity aberration.

Whereas the graph of Fig. 40 shows the absolute values of the cardinal distances g and f for any spread of the incident electron velocity, another way of describing the velocity qualities of the lens is given by derivation of the differential aberrations.

For slight variation of the incident electron voltage we can express the displacement of the focus on the axis by

$$\Delta g = \frac{dg}{dB}\Delta B, \tag{109}$$

wherein the Δ's stand for a small change of the parameter. By Eq. 44 we correlate the change of B to the change of the incident voltage E_v

$$\Delta B = \frac{dB}{dE_v}\Delta E_v = \frac{\Delta E_v}{2Bp} = \frac{B^2 + Z^2}{2B}\frac{\Delta E_v}{E_v}, \tag{110}$$

wherein Eq. 43 also is used. On the other hand, differentiation of g from Eq. 58 yields

$$\frac{dg}{dB} = \frac{\sqrt{2}\cot\left[\sqrt{2}\sinh^{-1}\left(\frac{Z}{B}\right)\right]}{\sqrt{1+\left(\frac{Z}{B}\right)^2}} + \frac{2\frac{Z}{B}}{\sin^2\left[\sqrt{2}\sinh^{-1}\left(\frac{Z}{B}\right)\right]}. \tag{111}$$

If we substitute here for the sine and cotang their values from Eqs. 58 and 62, we obtain for the longitudinal velocity aberration of Eq. 109 the concise expression

$$\Delta g = \frac{1}{2}f\left(\frac{g}{f} + \frac{Z}{B}\frac{f}{B}\right)\frac{\Delta E_v}{E_v}. \tag{112}$$

Thus, the velocity displacement of the focus is proportional to the relative spread of the incident electron voltage and further directly depending on the values of back-focus and focal length ratios.

For example, with ratios $f/B \cong 2.1$ and $g/B = 0.6$, corresponding

to $Z/B = 1.0$, the differential velocity displacement of the back-focus is

$$\frac{\Delta g}{f} = \frac{1}{2}\left(\frac{0.6}{2.1} + 1 \cdot 2.1\right)\frac{\Delta E_V}{E_V} = 1.19\,\frac{\Delta E_V}{E_V}.$$

The change of the focal length with incident electron voltage is different from this value, since the principal plane is also depending on velocity, as indicated in Fig. 39. The differential aberration of f is

$$\Delta f = \frac{df}{dB}\,\Delta B. \tag{113}$$

Differentiation of Eq. 62 gives

$$\frac{df}{dB} = \frac{\sqrt{2}}{\sqrt{1 + \left(\frac{Z}{B}\right)^2}\,\sin\left[\sqrt{2}\,\sinh^{-1}\left(\frac{Z}{B}\right)\right]} + \frac{2\,\frac{Z}{B}\cos\left[\sqrt{2}\,\sinh^{-1}\left(\frac{Z}{B}\right)\right]}{\sin^2\left[\sqrt{2}\,\sinh^{-1}\left(\frac{Z}{B}\right)\right]}. \tag{114}$$

Substituting again the trigonometric functions from Eqs. 58 and 62, and using Eq. 110 for ΔB, we obtain for the aberration in focal length

$$\Delta f = \frac{1}{2} f\left(1 + \frac{Z}{B}\frac{g}{B}\right)\frac{\Delta E_V}{E_V}. \tag{115}$$

The numerical values of the above example give

$$\frac{\Delta f}{f} = \frac{1}{2}(1 + 1 \cdot 0.6)\,\frac{\Delta E_V}{E_V} = 0.80\,\frac{\Delta E_V}{E_V}.$$

This variation is smaller than the displacement of the focus, due to the shift of the principal plane.

We see from Eqs. 112 and 115 that both the velocity aberrations are depending on the focal length f as well as on the back-focus g. An approach to the blocking condition, $B = 0$, will make either aberration extremely large. On the other hand, the spread Δf of the focal length will be small for $g = 0$, the focus being in the lens surface, and even will vanish for $g = -0.61\,B$, the focus deep within the lens volume. The spread Δg of the back-focus, however, will not attain such small values.

10. HYPERBOLIC ABERRATION.

If the lens is built with equipotential boundaries in the region of the axis a hyperbolic aberration develops due to the hyperboloidal surfaces of the field. This type of defect is in some analogy to the "spherical aberration" of light-optical lenses.

In a parallel uniform electron beam of relatively large diameter

entering the lens as in Fig. 41, the edge rays will traverse the field through a longer axial distance $\bar{Z}$ than the paraxial rays of length Z do. Therefore, they will experience a relatively greater deflection and a displacement of their focus. The half-width of the lens outside the axis is, by Eq. 18,

$$\bar{Z} = \sqrt{Z^2 + \frac{\bar{r}^2}{2}}, \tag{116}$$

wherein $\bar{r}$ denotes the radius of the incident ray. The symbol $Z = \sqrt{\Phi/p}$ shall now be restricted to the half-width of the lens on the axis.

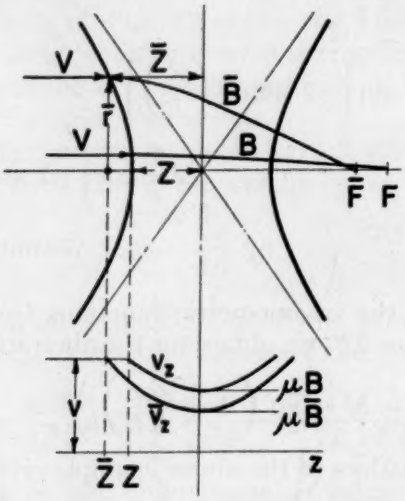

FIG. 41. Surface curvature of equipotential lens.

The transmission constant is depending on Z, as seen by Eq. 44. Thus, $\bar{B}$ will be smaller for extra-axial rays, namely

$$\bar{B} = \sqrt{\frac{E_V}{p} - \bar{Z}^2}. \tag{117}$$

Substituting $\bar{Z}$ from Eq. 116 and then B from Eq. 44 yields

$$\bar{B} = \sqrt{B^2 - \frac{\bar{r}^2}{2}}, \tag{118}$$

wherein the symbol B shall now be restricted to the transmission constant along the axis. Thus, for extra-axial rays $\bar{B}$ depends upon the radius of incidence.

A parallel incident edge ray, as in Fig. 41, will leave the lens at a smaller radius than it had at entrance. Thus, the exit abscissa will be smaller than the entrance abscissa, and this will lead to an unsymmetrical behavior of the lens, which is outside the scope of this paper. There-

fore, we will consider here only the performance of symmetrical rays and central rays, as represented in Figs. 42 and 43. Both of these rays will pass through the same distance $\bar{Z}$ on the two sides of the lens.

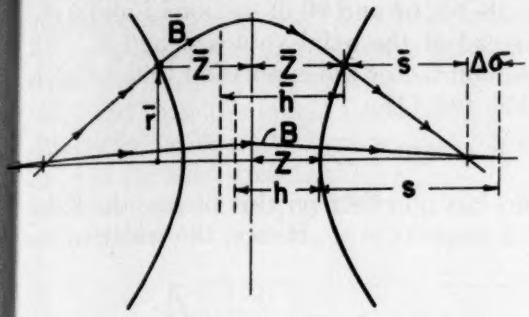

FIG. 42. Symmetrical ray in equipotential lens.

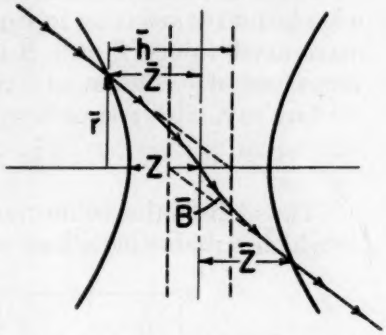

FIG. 43. Central ray in equipotential lens.

For increasing separation of the rays from the axis, the transmission constant $\bar{B}$ decreases, according to Eq. 118, and vanishes for a radius

$$r_o = \sqrt{2}B. \tag{119}$$

For greater radii the electrons will be reflected, and thus the radius r_o constitutes a natural limiting aperture. Substituting r_o into Eq. 118 yields

$$\frac{\bar{B}}{B} = \sqrt{1 - \left(\frac{\bar{r}}{r_o}\right)^2}. \tag{120}$$

The transmission constant, therefore, follows a circle diagram over the radius as indicated in Fig. 44.

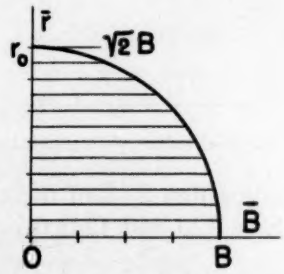

FIG. 44. Extra-axial transmission constant *versus* separation from axis.

Introducing the value of Eq. 119 into Eq. 116 yields

$$\frac{\bar{Z}}{B} = \sqrt{\left(\frac{Z}{B}\right)^2 + \left(\frac{\bar{r}}{r_o}\right)^2}. \tag{121}$$

For a radius $\bar{r}$ of 10 per cent of the limiting radius r_o the transmission constant decreases by $\frac{1}{2}$ per cent, for a radius of 20 per cent by 2 per cent

and for a radius of 30 per cent by 4.5 per cent. The same percentage increase occurs in the axial path length of the ray through the lens, if the ratio Z/B is taken as unity.

We now can determine the cardinal distances for the edge rays of a wide beam by inserting in Eqs. 58, 61, 62 and 80 of sections 5 and 6 the extra-axial values $\bar{Z}$ and $\bar{B}$ instead of the axial values Z and B. All these formulas contain as a common factor the expression (59) which is for any ray, with use of Eqs. 116 and 118,

$$\sqrt{\bar{B}^2 + \bar{Z}^2} = \sqrt{B^2 + Z^2}. \tag{122}$$

Thus, the finite beam radius has no effect on this factor, the value of which remains invariant with respect to $\bar{r}$. Hence, the width of the

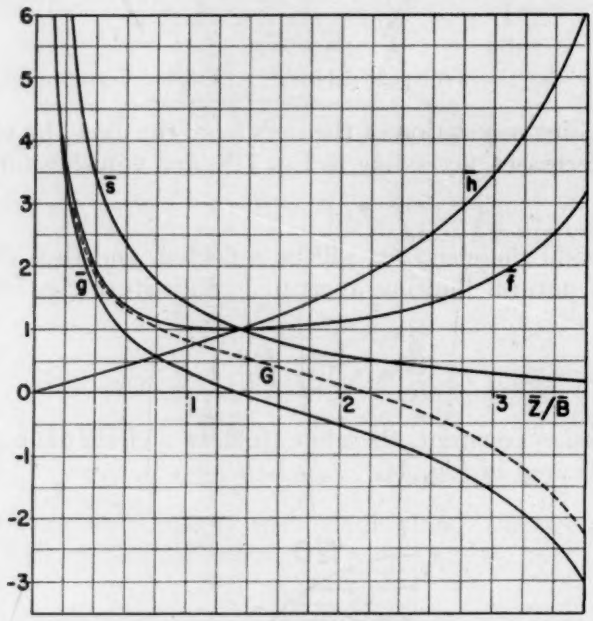

FIG. 45. Change of cardinal values with separation of ray from axis.

beam affects merely the argument $\bar{Z}/\bar{B}$ of the trigonometric-hyperbolic functions. With use of Eqs. 120 and 121, this is

$$\frac{\bar{Z}}{\bar{B}} = \sqrt{\frac{\left(\frac{Z}{B}\right)^2 + \left(\frac{\bar{r}}{r_o}\right)^2}{1 - \left(\frac{\bar{r}}{r_o}\right)^2}}. \tag{123}$$

For equal change of $\bar{r}/r_o$ this argument varies less with application of lenses thick in Z/B, than of thin lenses.

Figure 45 represents by the full-line curves the four characteristic

functions according to which $\bar{f}$, $\bar{g}$, $\bar{h}$, and $\bar{s}$ change if the argument $\bar{Z}/\bar{B}$ varies over any range. They show directly the longitudinal aberrations of the cardinal distances depending on $\bar{Z}/\bar{B}$ if any axial value Z/B is chosen. Only the focal length $\bar{f}$, due to its sine function, experiences a minimum at the point $\bar{Z}/\bar{B} = 1.35$, indicating a lens free of focal length defect. This ratio, incidentally, would bring the focus into the boundary of the lens, $\bar{g}$ being zero here. However, $\bar{g}$ and $\bar{h}$ vary even at this point and thus the image formation, as determined in addition to f by either g (Eqs. 70 and 72) or h (Eqs. 71 and 73) yet will not be perfect for both paraxial and edge rays.

The image formed by the edge rays has position and magnification both different from those of the paraxial image, as indicated by Fig. 46.

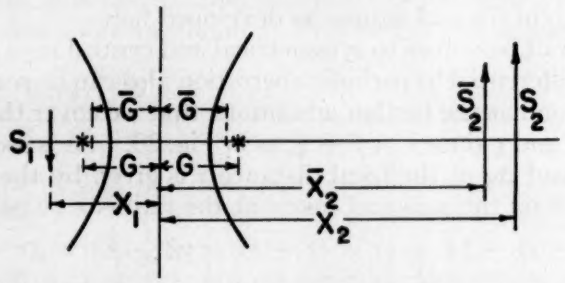

FIG. 46. Image formation determined by focal length and focal position.

In using Eqs. 70 and 72, we must note that the distances x and g are to be taken from the boundary of the lens, which is itself curved and thus is not suitable as a surface of reference. If we refer instead to the fixed center plane of the lens, as shown in Fig. 46, the new distances are X_1 and X_2 for object and image, and G for the back-focus, the focal length f remaining unchanged. The focal distance G to the center of the lens now is

$$G = Z + g = \sqrt{2}\sqrt{B^2 + Z^2} \times \left\{ \frac{Z/B}{\sqrt{2\left(1 + \left(\frac{Z}{B}\right)^2\right)}} + \cot\left[\sqrt{2}\sinh^{-1}\left(\frac{Z}{B}\right)\right] \right\}. \quad (124)$$

The factor in the brace is plotted as dashed curve in Fig. 45. Its rate of change is slightly smaller than that of g, since Z varies conversely to g.

Derived from Eqs. 70 and 72, the distance of the image from the center of the lens is

$$X_2 = G + \frac{f^2}{X_1 - G} \quad (125)$$

and the magnitude of the image is

$$S_2 = S_1 \frac{f}{X_1 - G}. \tag{126}$$

For the paraxial rays the values of f and G are to be taken with argument Z/B and for the edge rays with argument $\bar{Z}/\bar{B}$, determined from $\bar{r}/r_o$ by Eq. 123.

Parallel rays of incident radius $\bar{r}$ have always a smaller exit radius than $\bar{r}$, as shown by Fig. 41, and therefore their aberration will be substantially smaller than that of symmetrical rays. For the most part, the image is mainly formed by rays traversing the lens somewhere between the symmetrical and central rays, as seen by Fig. 16. Then, the effective aberrations of hyperbolic lenses will be below the margins of the formulas, curves and figures as developed here.

If we restrict ourselves to symmetrical and central rays as in Figs. 42 and 43, the differential hyperbolic aberration also can be readily derived. This restriction has the further advantage that we cover the aberrations due to both f and g since $s = f + g$, as in Fig. 20. As is seen by Fig. 42, the axial spread $\Delta\sigma$ of the focal distance s is given by the difference of $(Z + s)$ taken on the axis and taken at the radius $\bar{r}$

$$\Delta\sigma = (Z + s) - (\bar{Z} + \bar{s}) = (s - \bar{s}) - (\bar{Z} - Z) = \Delta s - \Delta Z. \tag{127}$$

Herein, the change of Z counteracts favorably the change of s. From Eq. 116 we derive

$$\bar{Z}^2 - Z^2 = \frac{\bar{r}^2}{2} = (\bar{Z} + Z)(\bar{Z} - Z) \tag{128}$$

and, therefore, in sufficient approximation

$$\Delta Z = \frac{\bar{r}^2}{4Z} = \frac{1}{2}\left(\frac{\bar{r}}{r_o}\right)^2 \frac{B^2}{Z}, \tag{129}$$

where in the last expression the blocking radius r_o of Eq. 119 is introduced.

For small aberrations, Δs may be expressed by the derivative of s with respect to the quotient Z/B, both these parameters contributing to the variation,

$$\Delta s = \frac{ds}{d(Z/B)} \cdot \Delta\left(\frac{Z}{B}\right). \tag{130}$$

The difference $\Delta(Z/B)$ may be derived from Eq. 123 analogous to the development of ΔZ above, yielding in good approximation

$$\Delta\left(\frac{Z}{B}\right) = \frac{\bar{Z}}{\bar{B}} - \frac{Z}{B} \cong \frac{1}{2}\left(\frac{\bar{r}}{r_o}\right)^2 \left(\frac{B}{Z} + \frac{Z}{B}\right). \tag{131}$$

When differentiating Eq. 80 expressing s, we must note that according to Eq. 122 the value of the first factors remains invariant and thus only

the cotang is variable with Z/B. This gives

$$\frac{ds}{d(Z/B)} = \frac{B}{\sin^2\left[\frac{1}{\sqrt{2}}\sinh^{-1}\left(\frac{Z}{B}\right)\right]}. \tag{132}$$

Substituting now Eqs. 129, 131, and 132 into Eq. 127, we obtain as total hyperbolic aberration

$$\frac{\Delta\sigma}{B} = \frac{1}{2}\left(\frac{\bar{r}}{r_o}\right)^2 \cdot \frac{B}{Z}\left\{\frac{1+\left(\frac{Z}{B}\right)^2}{\sin^2\left[\frac{1}{\sqrt{2}}\sinh^{-1}\left(\frac{Z}{B}\right)\right]} - 1\right\}. \tag{133}$$

The change of this longitudinal aberration with ratio Z/B is shown in Fig. 47. It has a flat minimum at $Z/B = 2.0$, giving a magnitude 2.89

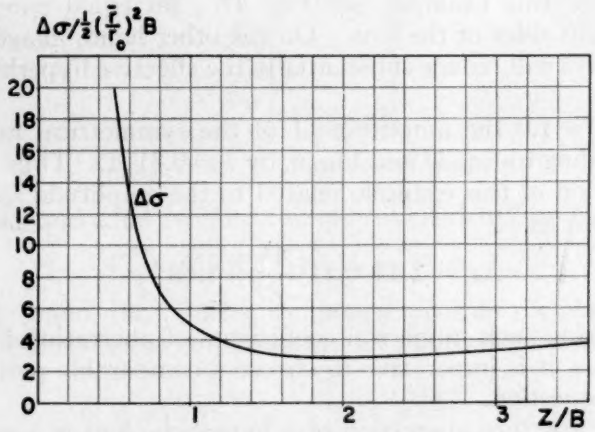

FIG. 47. Hyperbolic aberration depending on lens thickness.

for the factor which varies with Z/B. Hence the optimum lens thickness with respect to hyperbolic aberration is much larger than the optimum thickness with respect to focal length, see Eq. 63 and Fig. 17. This is due to the decreasing curvature of the lateral hyperboloids with thicker lenses. For values of Z/B beyond the range of Fig. 47 the value of $\Delta\sigma$ repeats to descend to further minima which, however, are higher than that shown in the figure.

The trigonometric sine can be transformed into a cotang and thus the contents of the brace in Eq. 133 develop to

$$\frac{1+\left(\frac{Z}{B}\right)^2}{\sin^2\left[\frac{1}{\sqrt{2}}\sinh^{-1}\left(\frac{Z}{B}\right)\right]} - 1 = \left(\frac{Z}{B}\right)^2 + \left(1+\left(\frac{Z}{B}\right)^2\right)\cot^2\left[\frac{1}{\sqrt{2}}\sinh^{-1}\left(\frac{Z}{B}\right)\right]. \tag{134}$$

Substituting herein the focal distance of the symmetrical ray by Eq. 80, we obtain as concise formulation for the hyperbolic aberration

$$\Delta\sigma = \Delta f + \Delta g = \frac{1}{2}\left(\frac{\bar{r}}{r_o}\right)^2\left(Z + \frac{1}{2}\frac{s^2}{Z}\right). \tag{135}$$

This refers to the symmetrical ray and to the central ray of equal incident radius.

If we assume, as an example, $Z = 1.0B$, $f = 2.1B$ and $s = f + g = 2.7B$ and substitute for r_o the value of Eq. 119, the longitudinal aberration is

$$\Delta\sigma = \frac{1}{2}\frac{\bar{r}^2}{2B^2}\left(1.0B + \frac{1}{2}\cdot\frac{2.7^2}{1.0}B\right) = 1.16\frac{\bar{r}^2}{B} = 2.44\frac{\bar{r}^2}{f}.$$

This is a favorably small numerical value, particularly if we note that it covers the defects both in f and in g. The possible minimum value is less than $\frac{1}{2}$ of this example, see Fig. 47. An equal spread $\Delta\sigma$ will appear on both sides of the lens. On the other hand, image formation by parallel rays will reduce substantially the effective hyperbolic aberration.

For $Z/B = 1.0$ the amplitude A of the symmetrical ray is determined, according to Eq. 33 and Fig. 6, by $\bar{r} = 0.81\,A$. Thus, the hyperbolic aberration of this example related to the amplitude radius of the ray will appear as

$$\Delta\sigma = 2.44\cdot 0.81^2\frac{A^2}{f} = 1.60\frac{A^2}{f}.$$

When discussing such numerical coefficients of aberration for different electron lenses, it is imperative to choose a comparable position of the apertures in question.

Since the aperture aberration of a hyperbolic lens is a pure surface effect due to the curvature of the lateral boundaries it should be possible, theoretically, to exclude this defect by using lateral electrodes of plane parallel shape so far as the transparent electronic apertures extend. These, however, either should be fed to secure a correct distribution of potential, as in Eq. 12, or they will cause a slight distortion of the hyperbolic field structure which may give rise to a certain aberration of its own.

If, on the other hand, the lens is built with geometrical openings in the lateral hyperboloids, their aberration must be added to the surface defect of the main lens field. This supplementary aberration is greatly dependent on the performance of the electric field within the opening and may be larger or smaller, and even of opposite sign, than the main field aberration.

11. ANGULAR ABERRATION.

So far we have supposed that the axial velocity of the electron rays incident to the lens is independently given, as it suggests itself by the

solutions of the trajectories in Eqs. 30 and 31, different in character in the z and r direction. This condition is satisfied by homogeneous rays impinging in a parallel beam.

However, rays emitted from object points close to the lens as in Fig. 48 will have different axial velocity components, depending on the angle β of emission, even if the absolute velocity V over the entire central bundle of rays should be the same. This behavior leads to an imaging defect which in light-optics also would fall into the class of "spherical aberration."

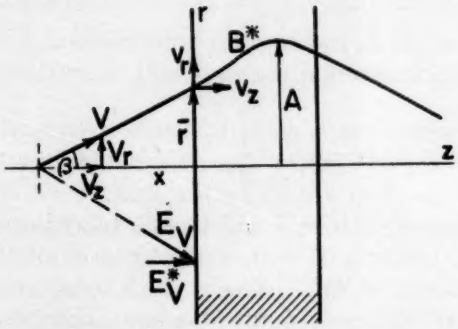

FIG. 48. Angular ray entering electron lens.

The radial and axial velocity components emitted are for each ray

$$V_r = V \sin \beta; \qquad V_z = V \cos \beta. \tag{136}$$

On the other hand, the velocity components within the lens, correlated by Eqs. 38 and 39 to the amplitude A and the transmission constant B, are

$$v_r = \nu\sqrt{A^2 - \bar{r}^2}; \qquad v_z = \mu\sqrt{B^2 + Z^2}. \tag{137}$$

At the boundary of the lens the respective velocity components coincide and thus, for an object on the axis, there is

$$V \sin \beta = \nu\sqrt{A^2 - \bar{r}^2}; \qquad V \cos \beta = \mu\sqrt{B^{*2} + Z^2}. \tag{138}$$

Herein, $\bar{r}$ is the radius of incidence of the ray considered, and B^* designates the transmission constant of this ray of angular incidence, which is smaller than the paraxial constant B. The value of the extra-axial transmission constant results from the second Eq. 138 as

$$B^* = \sqrt{\left(\frac{V}{\mu}\right)^2 \cos^2 \beta - Z^2}. \tag{139}$$

For paraxial rays, we have with $\beta = 0$ and corresponding to Eqs. 42 and 43, the simple correlation

$$\left(\frac{V}{\mu}\right)^2 = \frac{E_V}{p} = B^2 + Z^2. \tag{140}$$

Therefore, the angular transmission constant B^* can be expressed by

$$B^* = \sqrt{(B^2 + Z^2)\cos^2\beta - Z^2} \tag{141}$$

or, with use of Eqs. 26 and 140, as

$$B^* = \sqrt{\frac{E_V}{E}\left(Z^2 + \frac{R^2}{2}\right)\cos^2\beta - Z^2}. \tag{142}$$

This shows directly the dependence on the paraxial ratio of velocity voltage, on the incident angle of the ray and on the geometrical dimensions of the lens.

For a certain angle β_o the angular transmission constant will vanish and for greater incident angle the rays will be reflected. The blocking value is given by

$$\cos\beta_o = \frac{Z}{\sqrt{B^2 + Z^2}} \quad \text{or} \quad \tan\beta_o = \frac{B}{Z}. \tag{143}$$

For example, a lens of $Z/B = 1$ will have a blocking angle of $\beta_o = 45°$. A very thin lens, towards $Z = 0$, will transmit all the diverging rays up to an angle near $\beta_o = 90°$. A very thick lens, towards $Z = \infty$, will reflect with $\beta_o = 0°$ the rays of any incident angle.

The tangent of the emission angle is geometrically, from Fig. 48, and analytically, from Eqs. 138 and 141,

$$\tan\beta = \frac{\bar{r}}{x} = \frac{\nu}{\mu}\sqrt{\frac{A^2 - \bar{r}^2}{(B^2 + Z^2)\cos^2\beta}}, \tag{144}$$

wherein x designates the distance of the object from the boundary of the lens. This formulation allows to determine the amplitude of the angular rays within the lens field. We obtain from the first and last expression (144), with use of Eq. 32,

$$\sin\beta = \frac{1}{\sqrt{2}}\sqrt{\frac{A^2 - \bar{r}^2}{(B^2 + Z^2)}}. \tag{145}$$

If then, $\sin\beta$ is expressed by the first and second term of Eq. 144, there results

$$A = \bar{r}\sqrt{1 + 2\frac{B^2 + Z^2}{x^2 + \bar{r}^2}}. \tag{146}$$

This amplitude is always larger than the incident radius $\bar{r}$. For example, an object before a lens at $x = Z = B$ yields, if $\bar{r}$ is small as compared to x,

$$A = \bar{r}\sqrt{1 + 2\frac{1 + 1^2}{1^2 + 0^2}} = \sqrt{5}\,\bar{r} = 2.24\bar{r}.$$

Thus, the amplitude of such a ray would be more than twice the radius $\bar{r}$.

Since the transmission constant decreases with increasing angle of incidence there will occur an angular aberration of the extra-axial rays. This defect is caused solely by the gradual decrease of the axial velocity component. Hence, the magnitude of the angular aberration in f, g, and h can be determined from our former equations for the velocity aberration by use of the angular transmission constant B^* of Eq. 141 or 142.

Or, we may directly use the axial component E_V^* of the extra-axial velocity voltage. According to the defining Eq. 41 the voltage is proportional to the square of the velocity and therefore is for angular rays, corresponding to the second Eq. 136,

$$E_V^* = E_V \cos^2 \beta. \tag{147}$$

Thus, for a bundle of rays emitted from a point on the axis, this velocity aberration is substantially depending on the angle β of incidence. Using Eq. 147 for the reduced axial voltage of the inclined rays we can apply the curves of Fig. 40 for obtaining the distribution of the cardinal values over the angle of incidence.

For direct use as the main abscissa of Fig. 40, we determine the ratio of any axial voltage component to the blocking velocity voltage by substituting Eq. 143 into Eq. 107, yielding

$$\frac{E_V^*}{E_{V0}} = \frac{E_V^*}{E_V} \cdot \frac{E_V}{E_{V0}} = \left(\frac{\cos \beta}{\cos \beta_0} \right)^2. \tag{148}$$

Thus, the angle β related to the blocking angle β_0 is decisive.

The differential angular aberrations also can readily be derived. Equations 112 and 115 show that the velocity aberrations are determined by the relative axial voltage variation of the incident rays. This deviation is here, with use of Eq. 147,

$$\frac{\Delta E_V}{E_V} = \frac{E_V - E_V \cos^2 \beta}{E_V} = 1 - \cos^2 \beta = \sin^2 \beta. \tag{149}$$

Hence, the differential angular aberration will be:

for the back-focus

$$\Delta g = \frac{1}{2} f \left(\frac{g}{f} + \frac{Z}{B} \frac{f}{B} \right) \sin^2 \beta \tag{150}$$

and for the focal length

$$\Delta f = \frac{1}{2} f \left(1 + \frac{Z}{B} \frac{g}{B} \right) \sin^2 \beta. \tag{151}$$

Both these defects are depending on the sine-square of the angle of incidence.

Now, $\sin \beta$ is given by Eq. 145. Substituting therein r^2 from Eq. 146

yields

$$\sin^2\beta = \frac{A^2}{x^2 + r^2 + 2(B^2 + Z^2)}. \tag{152}$$

With the values of our former examples, $x = Z = B$ and $f = 2.1B$, and neglecting in the denominator r^2 as small compared to x^2, there results

$$\sin^2\beta = \frac{(A/B)^2}{1^2 + 2(1 + 1^2)} = \frac{1}{5}\left(\frac{A}{B}\right)^2 = 0.88\left(\frac{A}{f}\right)^2.$$

Thus, the angular aberration is with the same values as chosen after Eq. 112:

for the back-focus

$$\Delta g = 1.19 \cdot 0.88 \frac{A^2}{f} = 1.05 \frac{A^2}{f},$$

and for the focal length

$$\Delta f = 0.80 \cdot 0.88 \frac{A^2}{f} = 0.70 \frac{A^2}{f}.$$

Related to the incident radius r instead of the amplitude radius A of the rays, the aberrations would appear, with use of the value $A^2 = 5r^2$ formerly obtained, as $5.3r^2/f$ and $3.5r^2/f$, respectively. Compared with the hyperbolic aberration as in the example after Eq. 135, but taken twice for the two sides of the lens, we see that the angular aberrations for $x = Z$ are of the same order of magnitude as the hyperbolic aberrations maximally occurring.

When comparing the numerical values of aberration as obtained here under the conditions stated, with values published in the literature (7), it should be noted that most of the latter data are limited to the spread of the focal length Δf and disregard the spread of the back-focus Δg. For thick lenses, however, Δg is different from Δf and is more important for the definition of the image. As realized from the minima of focal length in Figs. 40 and 45, it would be possible in principle for the lenses here considered to reduce to zero the aberrations Δf, both with respect to velocity voltage and radius of surface aperture. This would require a lens thickness near to $Z/B = 1.5$ for both of the defects. However, the spread in back-focus, Δg, would remain, thus retaining a defect in position and magnification of the image as seen by Eqs. 70 and 72.

The magnitude of our various aberrations is in the general order of those of the best electron lenses theoretically determined in the literature (7). The coefficient of r^2/f usually obtained for good lenses varies from 30 to 3 and very rarely down to 0.3, figures which are, however, always related to the spherical aberration Δf alone, and refer to various positions of r within or without the lens.

It seems to be possible to compensate to a substantial degree the

surface and angular aberrations of the main hyperbolic lens field by a suitable structure of the electrostatic field in the lateral openings.

Such a hyperbolic electron lens was built and measured[3] in direct operation by a method derived from the lattice test as published by Spangenberg and Field (5). This yielded an aberration coefficient for Δf related to r^2/f of the order of 0.3 within the range of the possible errors of observation. This appears as a very small experimental value, indicating that the surface and angular aberrations of the main field were materially reduced.

12. TWO-DIMENSIONAL FIELD.

For a number of applications plane fields are employed acting on electron or ion rays like optical cylinder-lenses. If the field distribution

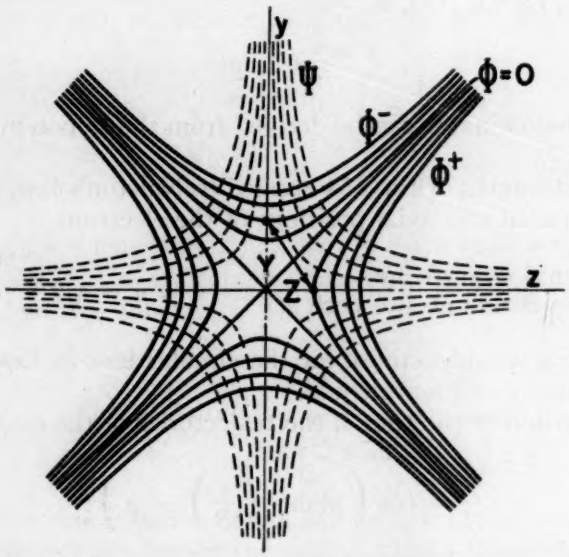

FIG. 49. Equipotential hyperbolas and field lines of cylinder lens.

is hyperbolic, as shown in Fig. 49, its lens performance can be readily treated analytically. The potential and stream functions of such a field are

$$\Phi = p(z^2 - y^2); \qquad \Psi = 2pyz, \tag{153}$$

wherein y and z denote the coordinates and the constant p determines the power of the field. Equipotential lines and stream lines are ordinary hyperbolas, one system at an angle of 45° with respect to the other. The asymptotes of zero potential are under 45°, in contrast to the nearly 55° in the case of rotational symmetry.

[3] This was performed by Drs. G. Fleming and R. Rempfer at the Laboratories of the Farrand Optical Co., Inc.

The field strengths as derived by Eq. 1 from Eqs. 153 are

$$\mathfrak{E}_y = 2py; \qquad \mathfrak{E}_z = -2pz. \tag{154}$$

Thus, each field strength is proportional to its own coordinate and is independent of the other coordinate. Hence, the electron trajectories can be determined rigorously.

Derived from the first Eq. 153, the voltage between two equipotential hyperbolas of opposite potential is

$$E = \Phi^+ - \Phi^- = p(Z^2 + Y^2), \tag{155}$$

wherein Z and Y denote the minimum distances of the respective hyperbolas from the origin. Thus, Z is the half-length and Y is the half-width of the cylindrical hyperbolic electron lens. The power of the field structure, by Eq. 155, is

$$p = \frac{E}{Z^2 + Y^2}, \tag{156}$$

wherein the denominator can be derived from the hypotenuse over $\overline{ZY}$, as in Fig. 49.

The field strengths of Eq. 154 applied to Newton's law, as in Eq. 27, yield for the radial and axial positions of the electrons

$$\left.\begin{aligned} y &= A\cos(\nu t - \varphi) \\ z &= B\sinh \mu t + C\cosh \mu t \end{aligned}\right\} \qquad \nu = \mu = \sqrt{2\frac{q}{m}p}. \tag{157}$$

These solutions resemble those for the circular lens in Eqs. 30 and 31, except that here ν and μ are equal.

By elimination of the time t, the trajectories of the electrons will be described by

$$\frac{y}{A} = \cos\left(\sinh^{-1}\left(\frac{z}{B}\right) - \varphi\right);$$

or

$$\frac{z}{B} = \sinh\left(\cos^{-1}\left(\frac{y}{A}\right) + \varphi\right), \tag{158}$$

if we limit ourselves to the transmitting case only, where C vanishes. Since the shape of these trajectories is independent of the amplitude A of the curve, all electron rays of parallel incidence upon one plane of the lens field will intersect at the same focal line of abscissa z. Hence, this two-dimensional hyperbolic lens field also is free from volume aberration for uniformly incident rays.

The radial and axial velocities of the electrons follow the same formulations as in the three-dimensional case, see Eqs. 38 and 39 and Fig. 9. Therefore, the same Eq. 44 develops for the transmission constant B in the two-dimensional case. Expressed by the power of the field, as

in Eq. 156, the transmission constant here is

$$B = \sqrt{\frac{E_V}{E}(Z^2 + Y^2) - Z^2} = \sqrt{\left(\frac{E_V}{E} - 1\right) Z^2 + \frac{E_V}{E} Y^2}. \quad (159)$$

For higher lens voltage E, this value decreases and is zero for

$$\left(\frac{E}{E_V}\right)_o = \frac{Z^2 + Y^2}{Z^2} = 1 + \frac{Y^2}{Z^2}. \quad (160)$$

Beyond this blocking condition, the cosh of Eq. 157 forms the solution and the field will reflect electron rays.

For unipotential fields, where the lens voltage E equals the incident electron voltage E_V, the transmission constant is simply $B = Y$, being given by half the width of the slit between the negative electrodes.

The slope of the electron rays within the lens field, derived from Eq. 158, is

$$\frac{dy}{dz} = -\frac{A}{B} \frac{\sin\left[\sinh^{-1}\left(\frac{z}{B}\right) - \varphi\right]}{\sqrt{1 + \left(\frac{z}{B}\right)^2}}. \quad (161)$$

For a symmetrical lens field of half-length Z the focal length is given by the subtangent of the trajectory, measured from the principal plane. This, similar to Eq. 62, is

$$f = \frac{A}{dy/dz} = \frac{B\sqrt{1 + \left(\frac{Z}{B}\right)^2}}{\sin\left[2 \sinh^{-1}\left(\frac{Z}{B}\right)\right]}. \quad (162)$$

Because of the sine function in the denominator, the focal length has a minimum value depending on the ratio Z/B and follows a general trend like that of Figs. 17 and 18. All the other cardinal values, as back-focus and principal points, can be derived in the same way and are different from those with circular field merely by a factor $\sqrt{2}$ in the numerator and under the sine.

If the field is limited by lateral equipotential hyperbolic cylinders permeable to electrons, a surface aberration will occur which is little higher than in the three-dimensional case because the curvature of the lateral hyperbolas is slightly greater in the two-dimensional case.

ACKNOWLEDGMENT.

I wish to express my great appreciation to Professor Emeritus H. E. Clifford whose criticism and advice have constantly helped me in concisely formulating my work.

LETTER SYMBOLS.

a = distance from origin on asymptote
A = amplitude of trajectories
B = transmission constant of lens
C = reflection constant of mirror
d = differential
E = lens voltage between electrodes
E_V = velocity voltage of incident electrons
$\mathcal{E}$ = field strength
f = focal length
g = back-focus, from lens surface
G = back-focus, from lens center
h = distance of principal plane from surface
p = power of hyperbolic lens field
q/m = charge/mass of electrons
r = radial coordinate
R = aperture radius of annular hyperboloid
s = focal distance of symmetrical ray
S = size of object or image
t = time
v = velocity of electrons
V = incident electron velocity
x = distance of object or image from lens surface
X = distance of object or image from lens center
y = transverse coordinate
Y = half-width of cylinder lens
z = axial coordinate
Z = half-length of lens field
α = angle of asymptotes
β = angle of incidence
Δ = finite difference
ν, μ = frequencies of motion
ρ = radius of curvature
σ = longitudinal aberration
φ = phase angle of trajectory
Φ = potential-function
Ψ = stream-function

REFERENCES.

(1) G. G. STOKES, "On the Steady Motion of Incompressible Fluids," *Trans. Cambr. Phil. Soc.*, Vol. 7, p. 439 (1842); *Math. and Phys. Papers*, Vol. 1, p. 1 (1880).

(2) R. RÜDENBERG, "Apparatus for Producing Images of Objects," U. S. Patent 2,058,914, Priority of May 30, 1931; "Apparatus for Influencing the Character of Electron Rays," U. S. Patent 2,070,319, Priority of May 30, 1931.

——, "The Early History of the Electron Microscope." (Contains excerpt of above patents.) *Jour. Appl. Phys.*, Vol. 14, p. 434 (1943).

(3) F. OLLENDORFF, "Potentialfelder der Elektrotechnik," (a book), p. 295, Julius Springer, Berlin, 1932.

(4) F. GRAY, "Electrostatic Electron Optics," *Bell Syst. Tech. Jour.*, Vol. 18, p. 1 (1939).

(5) K. SPANGENBERG AND L. M. FIELD, "Simplified Methods of Determining the Optical Characteristics of Electron Lenses," *Proc. I.R.E.*, Vol. 30, p. 138 (1942).

(6) C. H. BACHMAN AND S. RAMO, "Electrostatic Electron Microscopy," *Jour. Appl. Phys.*, Vol. 14, pp. 8, 69, 155 (1943).

(7) C. MARTON AND S. SASS, "Bibliography of Electron Microscopy," *Jour. Appl. Phys.*, Vol. 14, p. 522 (1943); Vol. 15, p. 575 (1944); Vol. 16, p. 373 (1945); Vol. 17, p. 759 (1946).

(8) J. M. LAFFERTY, "Electron Reflectors with Quadratic Axial Potential Distribution," *Proc. I.R.E.*, Vol. 35, p. 778 (1947).

OPTIMUM RATIO BETWEEN CRANK ARM AND CONNECTING ROD FOR SMOOTH OPERATION OF RECIPROCATING ENGINES.

BY

W. S. KIMBALL, Ph.D.[1]

INTRODUCTION.

Maximum speed of the crosshead in reciprocating engines was discussed in a previous paper [2] as a function of the angular position of the crank arm, and of the ratio of crank arm, r to connecting rod length, c. An expression for the maximum velocity $V_m = \dfrac{\omega r(n+1)}{\sqrt{n^2+n-1}}$ was found in terms of $n = x/\rho = c^2/y^2$, where $y = r \sin \theta_c$ gives the critical angular position of the crank arm for maximum crosshead velocity, and ω is the angular velocity of the crank arm or shaft, taken to be constant here and in the previous paper. Graphs of these maximum velocities plotted against the critical angle θ_c, and against the crank arm connecting rod ratio, r/c, showed (Figs. 4 and 5, footnote 2) them to differ in magnitude and position from V_t the crosshead velocity at the cycle position where crank arm and connecting rod are at right angles. As to both position and magnitude this difference was definite but very small for usual engineering values of the ratio r/c.

The present article is a special study of the magnitude of the crosshead *acceleration* maxima, of their angular position in the engine cycle (Fig. 1) and of how these maxima vary for different values of the ratio of the crank arm (throw of the crankshaft) to the length of the connecting rod (Fig. 2). Two curious results emerge from this study. The first is that for all ratios of this r/c slightly larger than the usual 1/4 (from 1/3.79 and ranging up to unity), there are three maxima per cycle instead of the two at the ends of the stroke as with simple harmonic motions. And two of these three maxima are positive crosshead acceleration maxima, that is, in direction away from the crankshaft and towards the cylinder, and occurring where the crank arm is at two symmetric positions *before* and *past* the position away from crank opposite the cylinder at angular position $\theta = \pi$, the stroke end, where positive acceleration is maximum for simple harmonic motions.

The second curious result is that these two positive crosshead acceleration maxima have a smallest (equal) value, or minimum under variations in r/c when the ratio of crank arm to connecting rod is given by $r/c = 1/2.8 = 0.357$, these occurring at cycle angle $\pm$ 132°,

[1] Lieutenant Commander, U. S. Naval Reserve; Department of Marine Engineering, U. S. Naval Academy, Annapolis, Md.

[2] W. S. Kimball, "Maximum Inertia Force and Maximum Speed of the Crosshead in Reciprocating Engines," JOURNAL FRANKLIN INST., Vol. 242, p. 309, October, 1946.

TABLE I.

$\rho=\frac{r^2}{c^2}$	$\sqrt{\rho}=\frac{r}{c}$	$u=\frac{y^2}{c^2}=\sin^2\alpha$	$z=\frac{y^2}{r^2}=\sin^2\theta$	$\sin\theta$	θ	Max. Positive Acceleration $\frac{V_m'}{\omega^2 r}$	Min. Positive Acc. at, $\theta=\pi$ $\frac{V''}{\omega^2 r}=1-\sqrt{\rho}$	Positive Acc. at $\theta=\pi/2$ $\frac{V'}{\omega^2 r}=\frac{1}{\sqrt{\frac{1}{\rho}-1}}$
						Eq. (20)	Eq. (12)	Eq. (13)
$\frac{1}{14.365}=0.0695=\frac{5-\sqrt{21}}{6}$	$\frac{1}{3.79}=0.262$	0	0	0	$\pi-0=\pi$	0.7368	0.7368	0.274
$\frac{1}{12}=0.08333$	$\frac{1}{2\sqrt{3}}=0.2886$	0.01683	0.20195	0.4494	153°18′	0.7158	0.7114	0.3015
$\frac{1}{10}=0.1000$	$\frac{1}{\sqrt{10}}=0.3165$	0.0372	0.3721	0.6100	142°25′	0.7023	0.6835	$\frac{1}{3}=0.3333$
$\frac{1}{9}=0.1111$	$\frac{1}{3}=0.3333$	0.0505	0.4545	0.6749	137°26.6′	0.6976	0.6666	$\frac{1}{\sqrt{8}}=0.3535$
$\frac{1}{7.837}=0.1276$	0.357	0.0703	0.551	0.7423	132°05′	0.6952	0.643	0.382
$\frac{2}{9}=0.2222$	0.4714	0.1818	$\frac{9}{11}=0.8181$	0.904	115°18′	0.737	0.5286	0.5347
$\frac{1}{4}=0.2500$	$\frac{1}{2}=0.5000$	0.2134	0.8536	0.9239	112°29.6′	0.7588	0.5000	$\frac{1}{\sqrt{3}}=0.5773$
$\frac{4}{9}=0.4444$	$\frac{2}{3}=0.6666$	0.4242	0.9657	0.9827	100°40′	0.9844	$\frac{1}{3}=0.3333$	0.8948
$\frac{2}{3}=0.6666$	0.8165	0.6632	0.99476	0.99736	94°10′	1.4501	0.1835	$\sqrt{2}=1.414$
$\frac{81}{100}=0.8100$	$\frac{9}{10}=0.9000$	0.80931	0.9991535	0.999565	91°42′	2.0819	$\frac{1}{10}=0.1000$	$\frac{9}{\sqrt{19}}=2.06433$
1.0000	1.0000	1.0000	1.0000	1.0000	90°	∞	0	∞

which is $\pm$ 48° away from the stroke end position $\theta = \pi$, where the positive maximum for simple harmonic motion occurs (see Fig. 3).

This ratio $r/c = 1/2.8$ is thus, in a certain sense, an optimum ratio, because minimum acceleration implies minimum jerk or inertia force for the crosshead and hence minimum engine wear and tear so far as these positive acceleration maxima are concerned. Also for this ratio, there is relatively small difference in the positive crosshead accelerations all the way around the outside half swing of the crank arm, thus making for smooth operation. Hence, $r/c = 1/2.8$ has been termed the optimum ratio for the smooth operation of reciprocating engines, although it refers only to positive crosshead accelerations, and negative

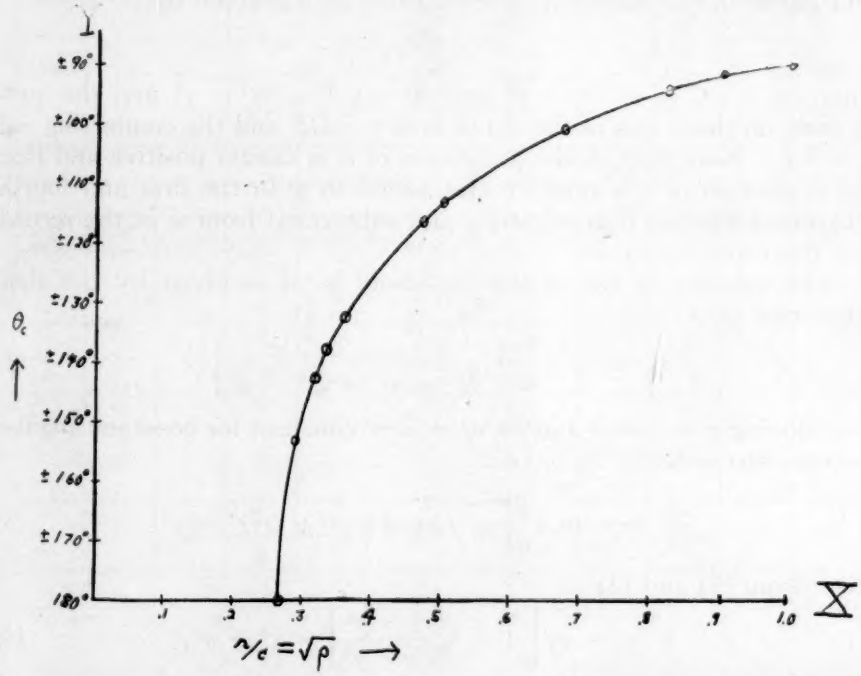

FIG. 1. Angular positions of the one or two positive acceleration maxima, showing where two occur at positions symmetric about $\theta = 180°$ for values of r/c greater than 1/3.79 = 0.2632.

acceleration maxima, Eq. 11, will be seen to have no minimum value, but increase linearly with r/c.

It does not appear that engines have been constructed with as large a ratio as this optimum $r/c = 1/2.8 = 0.357$, but its existence is here pointed out, and the position of its two smallest positive maxima at angular positions $\pm$ 48° away from the stroke end position $\theta = \pi$; and the fact that the magnitude of these maxima is only 69.52 per cent of the corresponding simple harmonic motion maximum, $\omega^2 r$ (see Table I) is here noted.

On the other hand, engines have been constructed where two positive acceleration maxima exist instead of a single one at $\theta = \pi$, as for simple harmonic motion. Thus the Liberty Motor, with a 7-in. stroke and a 12-in. connecting rod, has $r/c = 3.5/12 = 1/3.43 = 0.29$ and for this ratio Fig. 1 shows that positive acceleration maxima occur at $\pm 153°$ or at angular positions $\pm 27°$ away from $\theta = \pi$ at the end of the stroke. This engine thus has three crosshead acceleration maxima per cycle, including the negative one at $\theta = 0$ as well as the above two positive ones.

1. THE VELOCITY AND ACCELERATION OF THE CROSSHEAD.

Taking the center of the crankshaft as origin of coordinates, the position of the crosshead A, referring to Fig. 3 is given by

$$OA = x + w = \pm \sqrt{r^2 - y^2} + \sqrt{c^2 - y^2}, \tag{1}$$

where $x = OC = \pm \sqrt{r^2 - y^2}$ and $w = CA = \sqrt{c^2 - y^2}$ are the projections on the x axis of the crank arm $r = OB$ and the connecting rod $c = BA$. Note that w, the projection of c, is *always* positive and that the projection of r is positive and added to w in the first and fourth quadrants whereas it is negative, and subtracted from w in the second and third quadrants.

The velocity of the piston crosshead at A is given by the time derivative of (1):

$$V = -y\frac{dy}{dt}\left[\frac{\pm 1}{\sqrt{r^2 - y^2}} + \frac{1}{\sqrt{c^2 - y^2}}\right]. \tag{2}$$

Introducing $y = r \sin\theta$ and $d\theta/dt = \omega =$ constant for constant angular velocity of the shaft, we have:

$$\frac{dy}{dt} = r\cos\theta\frac{d\theta}{dt} = r\omega\cos\theta = \pm\omega\sqrt{r^2 - y^2}. \tag{3}$$

Then from (2) and (3)

$$V = -\omega y\left[1 \pm \sqrt{\frac{r^2 - y^2}{c^2 - y^2}}\right] = x' + w', \tag{4}$$

where we note that the signs of x' and w' check their tabulated values in Table I of the previous paper, the lower one of the paired signs always referring to the two quadrants at the left of the Y axis where x is minus and the upper of the paired signs referring to the two quadrants at the right of the Y axis where x is plus.

Likewise we may take the time derivative of (4) and obtain:

$$V' = -\omega\frac{dy}{dt}\left[1 \pm \frac{(y^4 - 2y^2c^2 + c^2r^2)}{\sqrt{(c^2 - y^2)^3(r^2 - y^2)}}\right], \tag{5}$$

or introducing (3):

$$V' = -\omega^2\left[\pm\sqrt{r^2 - y^2} + \frac{y^4 - 2c^2y^2 + c^2r^2}{(c^2 - y^2)^{3/2}}\right]. \tag{6}$$

Introduce

$$z = \sin^2\theta = y^2/r^2 \qquad \text{and} \qquad \rho = r^2/c^2. \tag{7}$$

Then

$$V' = -\omega^2 r\left[\pm\sqrt{1-z} + \frac{\rho^2 z^2 - 2\rho z + \rho}{\sqrt{\rho}(1-\rho z)^{3/2}}\right] = x'' + w''. \tag{8}$$

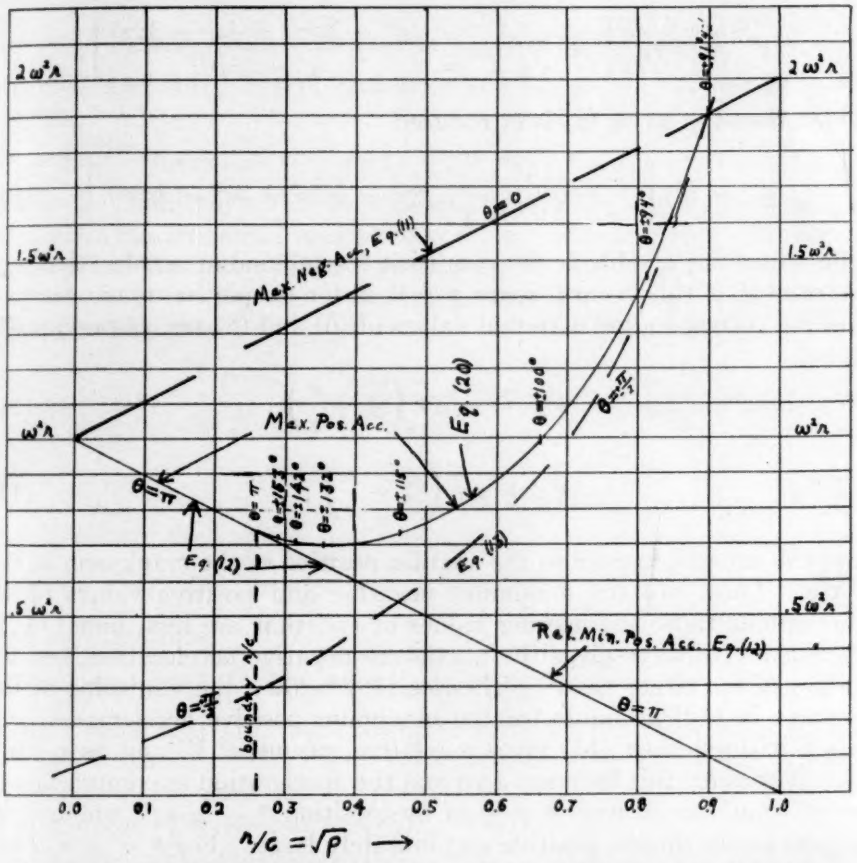

FIG. 2. Crosshead acceleration magnitudes as functions of r/c, the ratio of crank arm or throw of the crank, to connecting rod length, showing Eq. 20, Maximum Positive Acceleration, and Eq. 11, Maximum Negative Acceleration, and Eq. 12, Maximum, or Relative Minimum Positive Acceleration, and Eq. 13, for Positive Acceleration at $\theta = \pm\pi/2$, the limiting position of the maximum of Eq. 20 as the ratio r/c approaches unity.

Here the first term $x'' = -\omega^2 x$ is the simple harmonic motion formula for acceleration for the projection of r on OX and second one, w'' is the acceleration for the projection of the crank c, on OX and is seen to depend on ρ. The vanishing of (6) or (8) is the condition for maximum crosshead velocity treated in the previous [2] article. This vanishing occurs on the right of OY where x'' is minus and equal in magnitude to a positive w'' as given by (8) wherein hence $2\rho z = 2(y^2/c^2) = 2\sin^2\alpha$

is greater than $\rho + \rho^2 z^2$. A positive w'' always occurs for values of $\rho z = \sin^2 \alpha$ greater than the critical $\rho z = 1 - \sqrt{1 - \rho}$ which causes w'' to vanish.

2. CONDITION FOR MAXIMUM ACCELERATION OF THE CROSSHEAD.

The time derivative of (6) is

$$V'' = \omega^2 y \frac{dy}{dt}\left[\pm \frac{1}{\sqrt{r^2 - y^2}} + \frac{y^4 - 2c^2y^2 + 4c^4 - 3c^2r^2}{(c^2 - y^2)^{5/2}} \right], \qquad (9)$$

which becomes when (3) is introduced

$$V'' = \omega^3 y \left[1 \pm \sqrt{\frac{r^2 - y^2}{(c^2 - y^2)^5}} (y^4 - 2c^2y^2 + 4c^4 - 3c^2r^2) \right]. \qquad (10)$$

The vanishing of (10) is the condition for maximum acceleration and we note that this occurs where $y = 0$ as for simple harmonic motion, and the corresponding extremal values of (6) and (8) are, as previously[2] noted,

$$V_o' = -\omega^2 r \left(1 + \frac{r}{c} \right), \qquad (11)$$

$$V_\pi' = \omega^2 r \left(1 - \frac{r}{c} \right), \qquad (12)$$

and the subscripts refer to the angular position of the crank arm in the cycle. These are the maximum negative and positive values of V' throughout those engineering values of r/c, that are less than 1/3.79. Formula 11 always gives the maximum negative acceleration, but for values of r/c larger than 1/3.79 (see (16) below), the vanishing of the bracket in (10) accounts for the maximum positive acceleration, and when it does, then (12) gives a relative *minimum* V' and as r/c approaches unity this becomes zero and the acceleration maximum moves away from the position $\theta = \pi$ to the position $\theta = \pm \pi/2$ where it is, as previously shown, positive and infinitely large. For $\theta = \pm \pi/2$ the acceleration (6) or (8) is positive and given by

$$V'_{\pm \pi/2} = \frac{\omega^2 r^2}{\sqrt{c^2 - r^2}} = \omega^2 r \Big/ \sqrt{\frac{1}{\rho} - 1}, \qquad (13)$$

which is seen to become infinite when $r = c$, and $\rho = 1$. The present investigation shows how this comes about from the vanishing of the bracket in (10), with accompanying shift of the angular position of V_m' from $\theta = \pi$ to $\theta = \pm \pi/2$ as given by (13).

The condition for maximum V' is also given by the vanishing of its partial derivative with respect to $z = \sin^2 \theta$, which gives its maximum

under variations in the angle θ. Thus from (8) we have:

$$V_z' = \frac{\omega^2 r\sqrt{\rho}}{2}\left[\frac{\pm 1}{\sqrt{\rho - \rho z}} + \frac{\rho^2 z^2 - 2\rho z + 4 - 3\rho}{(1 - \rho z)^{5/2}}\right]. \tag{14}$$

When the crank arm is on the left of the Y axis, we use the lower sign in (14) and the bracket vanishes when

$$(1 - \rho z)^{5/2} = \sqrt{\rho - \rho z}(\rho^2 z^2 - 2\rho z + 4 - 3\rho).$$

Square this equality, cancel, transpose and factor out $1 - \rho$, and there remains:

$$\rho^4 z^4 + 2\rho^3 z^3 - 6\rho^2 z^2(1 + \rho) + \rho z(11 + 3\rho) + (1 - 15\rho + 9\rho^2) = 0. \tag{15}$$

This is the condition which determines the critical z (or angle θ) which maximizes the crosshead acceleration for a given ρ. Note that when the constant term $(1 - 15\rho + 9\rho^2)$ is zero, the equation is satisfied by $z = \sin^2\theta = 0$, so that the maximum occurs at $\theta = \pi$ and is given by (12). For this case

$$\rho = \frac{5 - \sqrt{21}}{6} = \frac{0.4174}{6} = 0.06956 = \frac{1}{14.365}, \tag{16}$$

$$\frac{r}{c} = \sqrt{\rho} = 0.26315 = \frac{1}{3.7914}.$$

Now introduce the variable

$$0 < u = \rho z = \frac{y^2}{c^2} = \sin^2\alpha < z < 1. \tag{17}$$

Then (15) becomes

$$u^4 + 2u^3 - 6u^2(1 + \rho) + u(11 + 3\rho) + (1 - 15\rho + 9\rho^2) = 0. \tag{18}$$

We may show that (15) and (18) have no real solutions when ρ is less than (16) because in this case the constant term $(1 - 15\rho + 9\rho^2)$ is positive. To see this, note that the positive term $11u$ is greater than all remaining negative terms put together, $-6u^2(1 + \rho)$:

$$11 > 6(1 + \rho) > 6u(1 + \rho). \tag{19}$$

This inequality obviously holds for $u < 1$ and ρ less than (16) and when (19) is multiplied by u, we have $11u$ greater than all negative terms combined, $-6u^2(1 + \rho)$; so that (15) never vanishes when $\rho = r^2/c^2$ is less than $(5 - \sqrt{21})/6$; that is, when $\sqrt{\rho} = r/c$ is less than $1/3.79$ according to (16).

Thus the bracket in (10) or (14) never vanishes when the ratio of crank arm to connecting rod length is less than $1/3.79$; and we note that this region includes the usual engineering practice where this ratio is about $1/4$. Thus the old Navy triple expansion reciprocating steam engines had about 1 to 4 for the ratio of crank arm to connecting rod.

Also some of the latest radial engines like R3350, used in the B-29's, which has a 14-in. connecting rod with a stroke of 6.312 in., or 3.156/14 = 1/4.43 for the ratio r/c in case of this comparatively long connecting rod. Maximum positive acceleration of the crosshead for the above cases is at $\theta = \pi$ and as for simple harmonic motion, there is also only this one angular position per cycle where maximum positive acceleration occurs.

The boundary ratio 1/3.79 is very close to 1/4 and many engines have been designed in recent years, having larger ratios than 1/3.79 between crank arm and connecting rod. Thus the Liberty motor has a

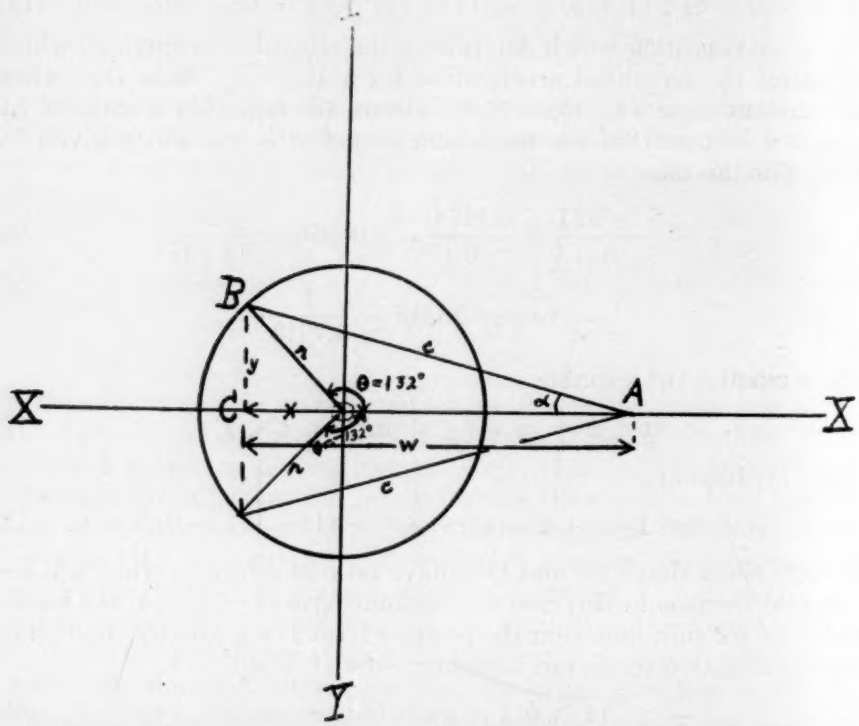

FIG. 3. The crank arm, r, and connecting rod, c, of ratio 1/2.8 shown at cycle angle ±132°, the positions of maximum positive crosshead acceleration per cycle, but the minimum value of this maximum under variations in r/c.

12-in. connecting rod and a 7-in. stroke, or 3.5-in. crank arm, or throw of the crank, with a ratio 3.5/12 = 1/3.43 = 0.29, which is larger than the above boundary ratio 1/3.79 between crank arm and connecting rod. Thus for this engine there are two equal positive acceleration maxima (as well as one negative maximum) at symmetric angular positions in the cycle at about $\theta = \pm 153°$ as shown near the lowest circle of Fig. 1, and determined by the vanishing of the bracket in (10) or (14) instead of by (12).

The Wright Whirlwind engine (Lawrence type) used by Lindbergh on his historic flight, had a 10.5-in. connecting rod and about 5.5-in. stroke or 2.75-in. crank arm or throw of the crank, giving a ratio $2.75/10.5 = 1/3.8$, which is almost at the boundary value $1/3.79$ separating the region where one positive acceleration exists at $\theta = \pi$ as in simple harmonic motion, from that in which two exist at symmetrical positions on either side of π as with the Liberty Motor.

3. MAXIMUM POSITIVE CROSSHEAD ACCELERATIONS.

The solutions of (15) or more easily (18) give the critical z (and hence angle θ) that maximizes the acceleration (6) or (8) for a given ρ, as this latter ranges from (16) to unity. These solutions may be obtained by Graeffe's method or by Horner's method. The maximum positive acceleration is then given by introducing these solutions into (6) or (8) using the minus (lower) sign in the first term since the crank arm is to the left of the Y axis where $\cos\theta$ is negative. Also introduce (17) for convenience in computations: Then

$$V_m' = \omega^2 r\left[\sqrt{1-z} - \frac{u^2 - 2u + \rho}{\sqrt{\rho}(1-u)^{3/2}}\right]$$

$$= \omega^2 r\left[\sqrt{1-z} + \frac{2u - u^2 - \rho}{\sqrt{\rho}(1-u)^{3/2}}\right]. \qquad (20)$$

For values of $r/c = \sqrt{\rho}$ ranging from 0.2632 to 1, Table I gives this maximum crosshead acceleration (20) and compares it with the smaller accelerations for each ρ at $\theta = \pm\pi/2$ and π. Note that for values of r/c greater than 0.8, as shown by the last three tabulated rows the maximum crosshead acceleration (20) approximates that for $\theta = \pm\pi/2$ its position when $\rho = 1$ as previously [2] shown.

4. MINIMUM VALUE OF THE MAXIMUM POSITIVE CROSSHEAD ACCELERATION.

Note from Table I that the smallest value of this maximum positive crosshead acceleration (20) is $V_m' = \omega^2 r$ (0.6952) and corresponds to $r/c = 0.357$ or $\rho = 1/7.837$. The condition for this minimum value of (20) under variations in ρ is given by setting the partial derivative of (8) with respect to ρ equal to zero (or the partial of (20) remembering that $u = \rho z$ by (17)). Thus:

$$\frac{\partial V'}{\partial \rho} = V_\rho' = \frac{\omega^2 r}{2\sqrt{\rho}}\,\frac{(\rho z^2 + 2z - 2\rho z - 1)}{(1-\rho z)^{5/2}} = 0 \qquad (21)$$

or

$$\left.\begin{aligned} \rho^2 z^2 + 2\rho z &= (2\rho z + 1)\rho \\ u^2 + 2u &= (1 + 2u)\rho \\ \rho &= \frac{u^2 + 2u}{1 + 2u} \end{aligned}\right\}. \qquad (22)$$

The condition for the minimum value under variations in ρ of the maximum crosshead acceleration given by (20) is the simultaneous vanishing of the partials of (8) with respect to z and with respect to ρ as given by (14) and (21); that is by solving (15), or more easily (18) simultaneously with (22).

When we introduce (22) into (18) we have a six degree equation in u, which has a double root of unity. Thus, when $(u-1)^2$ is factored out, there remains:

$$4u^4 + 8u^3 - 18u^2 - 13u + 1 = 0, \tag{23}$$

for the condition on u (and hence ρ by (22)) which minimizes (20). The solution of this equation by Horner's method gives the critical $u_c = 0.0703$ and the other critical variables and minimum $V_m' = \omega^2 r$ (0.6952) given in Table I.

Figure 2 shows the graphs of the positive acceleration of the crosshead for various values of the ratios r/c of crank arm to connecting rod, at angular crank arm positions away from and opposite the cylinder, $\theta = \pi$, at right angles $\theta = \pm \pi/2$ and at such positions as where maximum acceleration occurs.

Note that for $r/c < 0.2632$ that is, throughout usual practical engineering ranges the maximum curve coincides with the curve (linear) for $\theta = \pi$, and so, maximum positive crosshead acceleration occurs away from and opposite the cylinder, and on the other hand for large values of r/c, exceeding 0.8, this maximum acceleration differs from that at $\theta = \pm \pi/2$ by less than 3 per cent, being scarcely distinguishable on the graph, and occurring within 5° of the right angle position for crank arm and cylinder axis where $\theta = \pm \pi/2$.

A further fact about the extremal positive crosshead accelerations to note is that when the maximum V_m' moves away from position $\theta = \pi$ with $r/c = 0.263$, we still have zero for its rate of change (10) at $y = 0$, where $\theta = \pi$, which hence then is a position of minimum (relative) acceleration. But it is a rather flat minimum and differs only slightly from the maximum for values of r/c anywhere near usual engineering practice. Thus for $r/c = 0.357$ which determines the minimum of the maximum $V_m' = \omega^2 r$ (0.6952) as given by (20), at $\theta = \pm 132°$, the relative minimum at $\theta = \pi$, is $V_\pi' = \omega^2 r$ (0.643). The corresponding crosshead inertia forces will thus differ by less than 10 per cent which would indicate a steady and smoothly operating cycle in this region of positive accelerations with crank arm rounding the half circuit away from the cylinder, and point to $r/c = 0.357$ with its minimum V_m' above as an optimum ratio for the reduction of crosshead wear and tear due to positive acceleration.

The opinions or assertations contained in this article are the private ones of the writer and are not to be construed as official or reflecting the views of the Navy Department, or the Naval Service at large.

NOTES FROM THE NATIONAL BUREAU OF STANDARDS.*

MEASUREMENT OF RADIOACTIVE ISOTOPES.

The determination of the number of radioactive atoms in a sample of a radioactive isotope has become a matter of importance, because these isotopes not only have become an article of commerce but also are used in biological and medical experiments, and even in clinical treatment of diseases. Uniform quantitative results in all laboratories can be obtained only by using procedures that will yield absolute measurements or by the use of uniform standards of comparison that will give the same result whenever the determination is made.

The National Bureau of Standards has therefore issued standard samples of radioisotopes whose radioactivity has been accurately determined, and is planning to issue samples of additional radioisotopes as they become available. This follows logically the active role which the Bureau has long taken in the field of radioactive standards and measurements. It is furthermore in line with the Bureau's responsibility to furnish standards for precision measurement in all branches of the physical sciences.

Two factors are involved in the preparation and use of these samples. First, methods and standards that are correct in principle must be used. Second, a reasonable degree of accuracy must be attained in all steps of the process both of producing and of using the standards.

Essentially the measurement of a sample of radioisotope is the measurement of the number of radioactive atoms present. This, in turn, is dependent on the rate of disintegration, that is, the number of nuclear particles which are emitted in unit time from all atoms disintegrating within this interval of time. Counting the total number of disintegration particles, however, is not a simple procedure. The principal difficulty arises from the fact that these particles are emitted equally in all directions. It is therefore practically impossible to devise detecting equipment that will record all of them. Most of the difficulties in making quantitative determinations of radioisotopes, however, can be eliminated if standard sources of the isotope are available.

A standard source consists of a preparation of the isotope in a form convenient for use with the detector of radiation, and for which the disintegration rate is known from previous calibration. When the isotope to be measured is the same as that from which the standard is prepared, reliable results may be secured by observing only a few simple precautions. Other isotopes which have short half periods and a known disintegration scheme may also be measured with fair accuracy by

* Communicated by the Director.

means of beta-ray standards if it is known that a beta ray or a positron is emitted for every disintegration, and if the maximum energies of the beta-ray spectra of the standard and of the specimen are not too widely different.

In the case of those isotopes for which a disintegration scheme is lacking, or for which the mode of disintegration does not permit measurement of disintegration rates, an alternative method of comparing the activities of sources is available if the isotope emits gamma rays. Although this method does not give disintegration rates, it can, when properly applied, yield reliable comparisons of sources in various laboratories. It is limited, however, to comparisons of the same isotope. To secure reliable results, a standard instrument and standard geometry are necessary. The roentgen is a convenient unit of gamma radiation, which is defined without reference to the energy of the gamma ray. An ionization instrument properly designed to measure roentgens will therefore satisfy the requirements for a standard instrument. To determine the strength of a radioactive source the roentgens per unit time must be measured at a standard distance. On the basis of these considerations, Bureau scientists have proposed that the unit of time be one hour and the distance one meter, giving as a unit for comparison of gamma-ray sources the *roentgen per hour at a meter* (abbreviated *rhm*).

At the same time the name *rutherford* (*rd*) has been proposed for that quantity of radioisotope which disintegrates at the rate of a million disintegrations per second. This unit, which is smaller than the classical *curie*, can be specified exactly and independently of natural constants such as the rate of decay of radium, which is the basis for the definition of the curie. The National Bureau of Standards has adopted an arbitrary value of 3.700×10^{10} disintegrations per second for the curie when applied to isotopes other than members of the radium family.

The use of the rutherford in data presupposes that a disintegration rate has been measured and that this rate is expressed in disintegrations per second. This procedure removes all confusion regarding units and renders data from different laboratories comparable on an absolute basis.

EXPANSIVE CHARACTERISTICS OF HYDRATED LIMES.

It is highly important that a mortar or plaster after setting in place shall not undergo any appreciable change in volume, because volume changes frequently result in damage or even complete failure of the finished job. The National Bureau of Standards has been interested for some time in a widespread type of plaster failure, characterized by the formation of large blisters or bulges in the finished coat and caused by an increase in volume of the hardened plaster. Laboratory studies led to the conclusion that the expansion is due to a slow chemical change taking place in one of the chemical compounds that is naturally present

in many limes. As a result of these studies a limit for this constituent and others that might act in the same way has been included in recent specifications of the American Society for Testing Materials and the American Standards Association. The requirement is that the percentage of unhydrated oxides in hydrated limes shall not exceed 8 per cent by weight.

Recognizing that chemical composition alone does not always provide an indication of the soundness of hydrated lime, the Bureau continued the investigation to develop a suitable performance test. Because unsoundness does not usually show up for several years, an accelerated test has been proposed. The test involves preparation of a test bar by mixing the lime with portland cement, heating the bar (after it has set) in an autoclave, and measuring the expansion of the bar. An autoclave was specially modified to observe the behavior of test specimens during autoclaving.

Eighty commercial hydrated limes have been subjected to this treatment and to other tests for determining the effects of variables such as the amount of lime in the bars. In each case the relation between expansion and percentage of unhydrated oxides, the components that appear to cause this particular behavior, has also been determined. From these data, details of the test procedure have been worked out and a limit of expansion suggested.

HUMIDITY TEST APPARATUS.

A humidity test apparatus,[1] developed and built in the Mechanical Instruments Laboratory of the National Bureau of Standards, now makes available an instrument for research, calibration, and testing of hygrometers at temperatures below freezing. The use in recent years of radiosondes for the meteorological sounding of the atmosphere, an important acid in weather forecasting, has created a marked need for information on the performance of the humidity-sensing element in the radiosonde under conditions of flight. The humidity test apparatus was developed under the sponsorship of the Bureau of Ships, Department of the Navy, to provide an instrument for the investigation of radiosonde hygrometer elements at the temperatures and air velocities encountered during a flight.

The function of the humidity test apparatus is to produce air of known relative humidity at temperatures from 0° to −40° C. In the new divided flow, low temperature humidity test equipment developed by Arnold Wexler, a current of dry air is divided into two streams, one of which is maintained dry while the other is saturated with respect to ice; finally the two are recombined.

[1] For further technical details see, "Divided Flow, Low Temperature Humidity Test Apparatus," by Arnold Wexler, *J. Research NBS*, **40**, 479 (1948) RP1894.

A proportioning valve is used to divide the flow of moisture-free air in a known ratio. One part is passed through a saturator over a series of trays containing ice, until it is completely saturated. It is then mixed in a mixing chamber, with the other part that has been maintained dry, and allowed to exhaust through a test chamber into the atmosphere. The saturator, mixing chamber, and test chamber are kept immersed in a constant temperature bath. The hygrometer or other device, which is being subjected to air of known and constant humidity, is inserted into the test chamber.

The relative humidity in the test chamber is a function of (*a*) the fraction of air that passes through the saturator, (*b*) the total pressure in the saturator, (*c*) the total pressure in the test chamber, (*d*) the saturation pressure, and (*e*) the partial pressure of the water vapor in the test chamber. Under ideal conditions, which the apparatus closely approaches, all variables except one are eliminated, and the relative humidity becomes equal to the fraction of air that passes through the saturator.

The essential functional units of the apparatus are the drying system, the proportioning system, the humidifying system, the mixing chamber, the test chamber, the cooling system, and the thermoregulating system for temperature control.

The drying system serves to remove all water from the air entering the apparatus by freezing in a dry ice-varsol bath. The dry air then passes through the proportioning system, the major feature of which is the proportioning valve. This valve, which divides the air in a definite ratio, consists of six orifices of equal cross-sectional area so arranged that by a turn of the knob of the valve the incoming air can be divided to produce any of seven ratios, 0, 1/6, 1/3, 1/2, 2/3, 5/6, and 1. The ratio is the fraction of air entering the valve that emerges through one exit channel.

The two air streams, upon leaving the proportioning system, flow through the humidifying system in parallel channels, thermally in contact with one another to allow heat interchange and temperature equilibrium between the two streams. Saturation of one stream is accomplished by allowing it to pass over a series of staggered ice-filled trays while the other stream passes over an identical path of dry shelves. The dry and saturated air are centrifugally mixed in a mixing chamber and discharged into the atmosphere through a $1\frac{1}{8}$ in. inside diameter tube that serves as a test chamber. The saturators, mixing chamber and test chamber are immersed in a bath whose temperature is closely regulated.

The over-all performance of the humidity test apparatus has been established by a series of gravimetric moisture determinations. For the temperature range of 0° to −40° C. and for air velocities up to 1500 ft. per minute, this instrument produces air whose relative humidity is known within 3 per cent.

While particularly suited for the investigation and calibration of hygrometers, psychrometers, and development apparatus at temperatures below 0° C., the humidity test equipment may find further application in general research and testing where air of a known low dewpoint or moisture content is desired. With such apparatus, devices placed in the test chamber can be subjected to discrete and almost instantaneous changes in relative humidity. Lag studies may therefore be easily made. The velocity of the air passing through the test chamber can be adjusted to any value up to 1500 ft. per minute.

Although this instrument was designed primarily to fill a basic need in meteorology, the refrigeration and air-conditioning industries may also find it useful. In all these fields, humidity plays an important role. With the humidity test apparatus, it is now possible to calibrate readily and accurately the various humidity measuring instruments employed at low temperatures.

VARIABLE-RESISTANCE SPRING TRANSDUCER.

A highly sensitive mechano-electrical transducer, which transforms slight displacements into large changes of resistance, current, or voltage, is being developed by W. A. Wildhack and his associates of the National Bureau of Standards. The active element of the device is a helical or conical spring wound in such a way that the initial tension varies slightly along its length. Thus, when the ends of the spring are pulled apart, the turns separate one by one rather than simultaneously.

When the spring is entirely closed, it has an electrical resistance approximately that of a cylindrical tube. When it is completely open, its resistance is that of the total length of the coiled wire. Resistance can thus be varied over a wide range by stretching the spring. As the percentage change in resistance may be hundreds of times greater than the percentage change in length, displacements as small as 1/100,000 of an inch can be easily measured without the use of electrical amplifying devices. The spring transducer thus provides a sensitive means for conversion of any mechanical displacement to a change in an electrical quantity that can be precisely determined. When connected to another transducer which gives a mechanical displacement output (a bimetallic strip responding to temperature changes, for example), the combination gives an easily measurable electrical output. This type of use suggests numerous scientific and industrial applications, including strain gages, pressure elements, accelerometers, electric weighing devices, automatic temperature controls, dc-ac inverters, and voltage regulators.

The preferable construction for the transducer is a four-arm bridge of which each arm is a variable-resistance spring. An increase in applied tension elongates one pair of springs and shortens the other pair. The

resistive unbalance of the bridge, as indicated by a galvanometer, thus gives a measure of the displacement that has occurred. With this arrangement, since the voltage can be nearly reversed through the bridge, the output voltage can be theoretically twice the input voltage.

The variation of the initial tension of the spring along its length may be accomplished in several ways: by conical winding, by varying the angle of feed of the wire on a uniform mandrel, or by varying its tension as it is wound. For greatest sensitivity the variation in initial tension is made quite small. To decrease contact resistance between successive turns of the closed spring, a high average initial tension is built into the spring, and the turns are coated with 0.0001 in. of gold. Thus far, nickel-alloy wire has been mainly used, because of its high resistivity and small change of mechanical properties with temperature.

The new transducer is undergoing further development at the National Bureau of Standards as part of a project on basic instrumentation for scientific research supported by the Office of Naval Research.

THE FRANKLIN INSTITUTE.

MEDAL DAY MEETING.

WEDNESDAY, OCTOBER 20, 1948.

The Annual Medal Day Exercises of The Franklin Institute were held in conjunction with the Monthly Stated Meeting on Wednesday, October 20th. This annual affair had been held in April in previous years, but upon recommendation of the Committee on Science and the Arts the Board of Managers voted to hold it on the third Wednesday in October.

There were approximately 375 members and friends of the Institute who attended the Dinner and the presentation of awards.

A reception in honor of the Medalists was held prior to the Dinner. The unveiling of the portrait of our past president, Dr. Charles S. Redding, took place at this reception. Dr. and Mrs. Redding were present together with the artist, Lieutenant Colonel J. J. Capolino. Mr. Nalle officiated at the ceremony of the unveiling.

Mr. Guy Marriner, Director of Music of The Franklin Institute, played the National Anthem, which opened the evening's exercises.

Mr. Richard T. Nalle, president of The Franklin Institute, greeted the assembly in opening the programme.

Since Medal Day was also a Stated Monthly Meeting of The Franklin Institute, the minutes of the previous meeting, which was held in May, had to be approved as printed. There was no dissent.

Mr. Nalle then reported that the evening's two Franklin Medalists had been nominated by the Board of Managers for Honorary Membership in The Franklin Institute. Mr. Nalle presented their names to the membership for voting. The motion was made, seconded, and carried.

The programme and list of Medalists for this year are listed below, and detailed information will be found in a subsequent issue of the JOURNAL.

PROGRAMME

Reception for Medalists ..... THE HOSTESS COMMITTEE

National Anthem ..... GUY MARRINER

Dinner ..... MEDALISTS, OFFICIALS AND GUESTS

Toast to Benjamin Franklin ..... RICHARD T. NALLE, President

Greetings ..... RICHARD T. NALLE, President

Introduction of Former Medalists ..... THE PRESIDENT

The Institute in 1948 ..... HENRY BUTLER ALLEN, Secretary

Presentation of Awards ..... THE PRESIDENT

Advances in Virus Research ..... DR. WENDELL MEREDITH STANLEY

Progress in Aviation ..... DR. THEODORE VON KÁRMÁN

(Read by W. Laurence LePage, in the absence of Dr. von Kármán.)

MEDALISTS

Presentation of Cresson Medal (1848)

EDWIN H. COLPITTS, (*in absentia*)
Director
The Engineering Foundation

Presentation of Longstreth Medals (1890)

RALEIGH J. WISE
Telefax Research Engineer
The Western Union Telegraph Company

NICHOLAS F. ARONE
Switchgear Divisions Laboratory
General Electric Company, Phila.

EDWIN H. BRINK
Assistant Director of Research
Masonite Corporation

Presentation of Potts Medal (1906)

DAVID BIGELOW PARKINSON
Research Engineer
Bell Telephone Laboratories

CLARENCE ANDING LOVELL
Switching Research Engineer
Bell Telephone Laboratories

EUGENE J. HOUDRY
Founder
Houdry Process Corporation

Presentation of Levy Medals (1923)

JAN A. RAJCHMAN
Research Engineer
Radio Corporation of America Laboratories

WILLIAM H. CHERRY
Physicist
Radio Corporation of America Laboratories

Presentation of Henderson Medal (1924)

CHARLES DUNCANSON YOUNG
Vice President (Retired)
The Pennsylvania Railroad Company

Presentation of Wetherill Medal (1925)

WENDELL FREDERICK HESS
Head, Department of Metallurgical Engineering
Rensselaer Polytechnic Institute

Presentation of Ballantine Medal (1946)

RAY DAVIS KELL
Director of Television Research
Radio Corporation of America Laboratories

Presentation of Franklin Medals (1914) and Certificate of Honorary Membership

WENDELL MEREDITH STANLEY
Professor and Chairman of the Departments of Biochemistry
Director of the Virus Laboratory
University of California, Berkeley, California

THEODORE VON KÁRMÁN, (*in absentia*)
Professor of Aeronautics and Director of Guggenheim Aeronautics Laboratories
California Institute of Technology

COMMITTEE ON SCIENCE AND THE ARTS.

(*Abstract of Proceedings of Stated Meeting held Wednesday, October 13, 1948.*)

HALL OF THE COMMITTEE,
PHILADELPHIA, OCTOBER 13, 1948.

MR. WALTER C. WAGNER, *Acting Chairman*, in the Chair.

The following report was presented for final action:

No. 3192: Fowler Flap.

This report recommended the award of a John Price Wetherill Medal to Harlan D. Fowler, of Whittier, California, "In recognition of his many years of consistent endeavor directed toward a successful solution of the problem of variable lift airplane wings, culminating in the development of the Fowler Flap as an ingenious combination of variable wing area, variable wing camber and adjustable slot."

JOHN FRAZER,
Secretary to Committee.

MUSEUM NOTES

ACTIVITIES FOR SCHOOL YEAR 1948–49.

The work of the Educational Department is in full swing, booking reservations and conducting groups on visits to the Museum, Planetarium and Dairy Dell. In anticipation of the busy fall season, two separate mailings have been prepared and sent out to a mailing list which includes over 1500 schools and several hundred administrators. Student tickets and teachers' identification cards, in sufficient numbers to take care of the student enrollment and faculty of each school have been sent out, along with information concerning group visits.

The second mailing consisted of the schedule of special school demonstrations in the Fels Planetarium for the First Semester. Many reservations were made for these shows in the first week of school sessions, with one teacher asking, on the 14th of September, for a booking in the Christmas show.

Because of the extreme popularity of these planetarium shows, and the necessity in previous years of turning so many groups away, many additional lectures have been scheduled for this season. Demonstrations are now given on Tuesday, Wednesday, Thursday and Friday mornings and on Tuesday and Thursday afternoons.

The Department is continuing to sponsor, in cooperation with the Board of Education and Station WFIL, the school radio program "Science is Fun." In connection with this weekly program, a teachers' manual is prepared and mailed out to all schools on the mailing list. This manual is designed to help teachers in preparing their classes to listen more profitably to the broadcasts, and contains suggestions for experiments children can do at home or in the classroom, vocabulary, and material tying in study visits to The Franklin Institute with the subjects in the weekly radio programs. The 1948–49 manual was prepared and mailed out in the early part of the fall semester.

The Director of Education expects this year, as in the past, to have many conferences with teachers and department heads in connection with specialized teaching problems, and to continue to work with teachers colleges and schools of education.

Cooperation with the Philadelphia Science Council, the United Nations Youth Council and many other organizations will be continued this year.

Plans are being made with the cooperation of the *Philadelphia Inquirer* for a Science Fair in May, 1949. This will be held at The Franklin Institute and students in all schools in the Philadelphia area have been invited to plan exhibits. This will include primary grades through high school.

Another special program which has been planned for the Second Semester is a repetition of the Planetarium program in connection with Classics Week. In order to be able to accommodate more students this season, additional shows for Classics Week have been incorporated in the regular school planetarium schedule.

LIBRARY NOTES.

The Committee on Library desires to add to the collections any technical works that members would wish to contribute. Contributions will be gratefully acknowledged and placed in the library. Duplicates received will be transferred to other libraries as gifts of the donor.

Photostat Service. Photostat prints of any material in the collections can be supplied on request. The average cost for a print 9 × 14 inches is thirty-five cents.

The Library and reading room are open on Mondays, Tuesdays, Fridays, and Saturdays from 9 A.M. until 5 P.M., and Wednesdays and Thursdays from 2 P.M. until 10 P.M.

RECENT ADDITIONS.

ARCHITECTURE AND BUILDING.

MURDOCK, L. J. Concrete Materials and Practice. 1948.
VOSS, WALTER C. Fireproof Construction. 1948.

CHEMISTRY AND CHEMICAL TECHNOLOGY.

BRANDENBERGER, E. Grundlagen der Werkstoffchemie. 1947.
DAVIDSON, MARTIN. The Mid-twentieth Century Atom. 1946.
FLAGG, JOHN F. Organic Reagents Used in Gravimetric and Volumetric Analysis. 1948.
FREAR, DONALD E. H. Chemistry of Insecticides, Fungicides and Herbicides. 1948.
KIRSCHBAUM, EMIL. Distillation and Rectification. 1948.
LEWIS, WINIFRED. Thin Films and Surfaces. No Date.
PIERCE, WILLIS CONWAY AND HAENISCH, EDWARD L. Quantitative Analysis. Third Edition. 1948.
A Symposium on the use of Isotopes in Biology and Medicine. 1948.

ELECTRICITY AND ELECTRICAL ENGINEERING.

SMULLIN, LOUIS D. AND MONTGOMERY, CAROL G. Microwave Duplexers. 1948.
BORDEN, PERRY A. AND THYNELL, GUSTAVE M. Principles and Methods of Telemetering. 1948.
COOK, ARTHUR L. AND CARR, CLIFFORD C. Elements of Electrical Engineering. Fifth Edition. 1947.
CROFT, TERRELL. American Electricians' Handbook. Sixth Edition. 1948.
DÜNNER, ERNST. Einfuhrung in die Elecktrotechnik. 1947.
SKILLING, HUGH H. Fundamentals of Electric Waves. Second Edition. 1948.

ENGINEERING.

ANDERSEN, PAUL. Substructure Analysis and Design. 1948.
MARIN, JOSEPH. Strength of Materials. 1948.
WHITE, ALFRED H. Engineering Materials. Second Edition. 1948.

FOOD.

ANSON, M. L. AND EDSALL, J. T. Advances in Protein Chemistry. Volume 4. 1948.
CRUESS, WILLIAM VERE. Commercial Fruit and Vegetable Products. Third Edition. 1948.

GEOLOGY.

FOSTER, EDGAR E. Rainfall and Runoff. 1948.
MCKINSTRY, HUGH EXTON. Mining Geology. 1948.

MANUFACTURE.

FASSETT, F. G., Editor. The Shipbuilding Business in the United States of America. Two Volumes. 1948.
FOUTS, E. L. AND FREEMAN, T. R. Dairy Manufacturing Processes. 1948.
MCCARTHY, JAMES REMINGTON. A Matter of Time. 1947.

MATHEMATICS.

MAC ROBERT, T. M. Spherical Harmonics. Second Edition. 1947.

MECHANICAL ENGINEERING.

HAM, CLARENCE WALTER AND CRANE, E. J. Mechanics of Machinery. Third Edition. 1948.
LORENZI, OTTO DE. Combustion Engineering. 1948.
RAUH, KURT. Praktische Getriebelehre. Two Volumes. 1931–1939.
SEVERENS, WILLIAM H. AND DEGLER, HOWARD E. Steam, Air and Gas Power. 1948.

METALLURGY.

SISCO, FRANK T. Modern Metallurgy for Engineers. Second Edition. 1948.

ORDNANCE.

BURCHARD, JOHN E. Rockets, Guns and Targets. 1948.

PATENTS.

PALMER, ARCHIE M. Survey of University Patent Policies. 1948.

PHYSICS.

BRAILSFORD, F. Magnetic Materials. 1948.

DAVIDSON, MARTIN, Editor. The Gyroscope and its Applications. Second Edition. 1948.

DEN HARTOG, JACOB PETER. Mechanics. 1948.

POYNTING, JOHN H. AND THOMSON, JOHN J. A University Text-book of Physics. Volume One. 1947.

PLASTICS.

NAUTH, RAYMOND. The Chemistry and Technology of Plastics. 1947.

PUBLICATIONS RECEIVED.

The Elements of Physics, by Alpheus W. Smith, 745 pages, 16 × 23 cm., drawings, illustrations, and plates. New York, McGraw-Hill Book Co., Inc., 1948. Price, $4.50.

Thermodynamics, by Edward F. Obert. 571 pages, 15 × 24 cm., plates, drawings and tables. New York, McGraw-Hill Book Co., Inc., 1948. Price, $5.50.

Engineering Contracts and Specifications, by Robert W. Abbett. Second ed., 327 pages, 14 × 22 cm., tables. New York, John Wiley & Sons, Inc.; London, Chapman & Hall, Ltd.; 1948. Price, $3.75.

Fundamentals of Electric Waves, by Hugh Hildreth Skilling. Second ed., 245 pages, 15 × 24 cm., drawings. New York, John Wiley & Sons, Inc.; London, Chapman & Hall, Ltd.; 1948. Price, $4.00.

Introduction to Applied Mathematics, by Francis D. Murnaghan. 389 pages, 16 × 23 cm. New York, John Wiley & Sons, Inc.; London, Chapman & Hall, Ltd.; 1948. Price, $5.00.

Atomic Energy, by Karl K. Darrow. 80 pages, 14 × 22 cm., tables and illustrations. New York, John Wiley & Sons, Inc.; London, Chapman & Hall, Ltd.; 1948. Price, $2.00.

Climatic Accidents in Landscape-Making, by C. A. Cotton. 354 pages, 14 × 22 cm., drawings and illustrations. New York, John Wiley & Sons, Inc.; London, Chapman & Hall, Ltd.; no date. Price, $7.00.

Public Health Engineering, by Earle B. Phelps and Others. 655 pages, 14 × 22 cm., tables, drawings, and illustrations. New York, John Wiley & Sons, Inc.; London, Chapman & Hall, Ltd.; 1948. Price, $7.50.

The Mathematical Basis of the Arts, by Joseph Schillinger. 696 pages, 17 × 25 cm., charts and illustrations. New York, Philosophical Library., 1948. Price, $12.00.

Readings in the Physical Sciences, edited by Harlow Shapley and Others. 501 pages, 16 × 24 cm., drawings. New York, Appleton-Century-Crofts, Inc., 1948. Price, $3.00.

Symposium on Internal Stresses in Metals and Alloys, organized by The Institute of Metals. 485 pages, 14 × 22 cm., drawings, tables, and illustrations. London, The Institute of Metals., 1948. Price, 42s.

Handbooks of Textile Technology No. 3, The Identification of Textile Materials. 10 pages, 15 × 24 cm., illustrations and plates. Manchester, The Textile Institute, no date. Price, 5s (Paper).

BOOK REVIEWS.

INDUSTRIAL MANAGEMENT, by William R. Spriegel. Fourth edition, 656 pages, illustrations, 15 × 24 cm. New York, John Wiley & Sons, Inc., 1947. Price, $5.00.

The objective behind any serious attempt to analyze the factors in industrial management is to study those administrative and managerial policies that have been most effective, to understand the physical phases of production, and to discover the proper balance among the man-

agerial, physical and employee relationships. The fourth edition of this book, now at hand, uses this as a plan, and attempts to make its presentation in sympathy with the college student who desires to learn the latest practices and the theory behind them, and the executive who is interested in suggestions that may help him solve his current problems.

The work is laid out in a logical way, starting with organization structure involving types of organization, coordination, morale, product development and research, standardization, processes, and inspection. The plant and equipment are next taken up including the elimination of limiting or bottle-neck operations, production centers, layouts, internal transportation, the production line, materials handling, lighting, power, air conditioning, etc. Motion and time study is a subject treated as both an engineering and a personnel management function. The taking of time studies, establishing true values by time study and the utilization of time study data are given attention. An up-to-date and enlightening discussion is that on wage payment, particularly in the beginning devoted to the basis of industrial wages.

A similarly interesting section of the book is that which follows on buying, selling, and transportation. With regard to the sales department it is stated "The growth in the size and complexity of present day markets has forced management to give increasing attention to the organization of the sales force and to the formulation of policies to guide this organization." A considerable portion of the book is devoted to material production and control, and the final part of the book is on personnel administration and management. In the back of the book there are a bibliography and a comprehensive subject index.

The book covers a large field for the industrial manager as well as those in charge of the many departments under him. It is a thorough, clear, and modern presentation.

R. H. OPPERMANN.

THE MODERN METALLURGY OF ALLOYS, by R. H. Harrington. 209 pages, diagrams, tables, 14 × 21 cm. New York, John Wiley & Sons, Inc., 1948. Price, $3.50.

Dr. Harrington, who is research metallurgist for the General Electric Company, has spent twenty-five years in the field of metallurgy. During this time he became aware that there seemed to be a lack of basic structure in the knowledge of the subject. There were ample data on the "whats" of metallurgy, but little on the "whys." His purpose in this book has been to supply some of these "whys," thus providing a foundation for the data that have been compiled.

The author's approach is both logical and fundamental, following what he considers the relative importance of the various topics. One of his major contributions has been the classification of terminology. Metallurgy, only about forty years old as a science compared with centuries of practice, has been beset by a multiplicity of theories and an overlapping in terms. Dr. Harrington has endeavored to express but one meaning with each term, choosing that which he felt was best represented by the word.

His first chapter constitutes a discussion and definition of heat-treatment terms grouped according to the three main alloy fields: "(A), allotropic modifications as in the iron-carbon system; (B) the cold-worked solid solutions, exemplified by cold-rolled brasses; and (C) precipitation-hardening alloys with the recently popularized copper-beryllium alloys as an example."

In the second chapter he presents a classification of ten types of equilibrium diagrams, accompanied by other diagrams showing the relationship of cooling curves and physical properties. He discusses likewise eight groups of reactions in the solid state, which are basic to heat treatments. The next chapter considers the role of strain in reactions of the solid state in alloys.

An interesting table which Dr. Harrington has prepared forms the subject of "A Metallurgist's Periodic Table." This includes data on crystal structure, lattice constants, closest atomic approach, melting point, resistivity, atomic radius, and energy levels for the different elements. The viewpoints of the physicist and of the chemist on metals are next presented.

A reverse viewpoint is offered under the title "The Metallurgist Looks at the Physics and Chemistry of Alloying." Here Dr. Harrington considers four factors in the formation of binary alloys, namely—atomic size, crystal-structure bonding, periodic grouping, and type of

lattice. These four factors are then studied in connection with the alloys of the ten different binary alloy systems. A concluding chapter offers comments on porosity and particles.

In his correlation of practical data with modern theory, the author offers a presentation which should interest both the practical and theoretical metallurgist.

G. E. PETTENGILL.

Q. E. D. M. I. T. IN WORLD WAR II, by John Burchard. 354 pages, plates, 15 × 23 cm. New York, John Wiley & Sons, Inc., 1948. Price, $3.50.

An active participant himself, Mr. Burchard has written a comprehensive and readable account of the contributions of Massachusetts Institute of Technology toward winning World War II. The book is divided into several parts, each of which takes up a different phase of the activities.

After a brief introductory section, the author discusses M. I. T. contributions on a national level. Its men played a leading role in the various research—directing agencies as well as taking a part in the active research for the Army, Navy, and NDRC.

Then follows an account of the research carried on at M. I. T. itself. This was of various kinds, although the developments of the Radiation Laboratory have received perhaps the most attention in the public mind. Flash photos played an important role in the European invasion and Mr. Burchard discusses their wartime development in some detail as an example of some of the problems involved.

Another section points out that other M. I. T. men made their contribution by serving on the production front and on the psychological front. Not the least important activity was the continuance of the teaching function, as not only were there special courses for the Army and Navy, but there was the vital need of maintaining a continuing though diminished flow of trained engineers for the years ahead.

Mr. Burchard emphasizes that this is the record of only one institution and that it was paralleled by others. It is a fine record and one that adequately demonstrates the capacity of a private university to contribute to the nation's welfare as effectively in time of war as it does in time of peace.

G. E. PETTENGILL.

APPLIED THERMODYNAMICS, by Virgil Moring Faires. Revised edition, 480 pages, illustrations, 15 × 24 cm. New York, The Macmillan Co., 1947. Price, $4.75.

Textbooks are continually being revised, as experience in teaching dictates a more impressionable presentation, and in order to keep abreast of new knowledge. Each succeeding student, therefore, receives increasing benefits. The most successful textbooks are built on tried and improved theories of presentation. The book at hand is a revised edition and attempts to put forth the subject in a manner of conceptions which in many cases build up, one on the other, into a large integrated image. In doing this, liberties are taken to digress from the usual beaten path to enlist interest and give life and substance to an otherwise abstract theory.

There are twenty-three chapters in all. The first gives conceptions concerning the transformations of energy, the transfer of energy, the storage of energy, the first law of thermodynamics, and the consequent general energy equation. Immediately following this is a foreword to the student, placed here "because so few people read forewords." And it contains information that is workable and profitable regarding study habits. Then energy equations of a perfect gas and reversible non-flow processes of gases furnish a foundation for an understanding of thermodynamic cycles which follow. This deals with the Carnot and Ericsson cycles and important deductions regarding limitations of any power machine. At this point, the student is warned that it is necessary to master completely the analysis of cycles. The trend then leads into entropy and the second law of thermodynamics, internal combustion engines, compression and expansion of air, and the flow of gases which, by the way, is approached from the point of view of the energy equation only, excluding the general subject of fluid mechanics.

What may be called another section of the book starts with the subject of combustion and the products of combustion and proceeds through specific heats, liquids and vapors, processes

of vapors, to steam power plant and auxiliary apparatus. This is followed by the study of thermodynamic cycles used as standards of comparison, the reciprocating steam engine, and the flow of steam in nozzles and turbines. The final chapters of the book are devoted to refrigeration, mixtures of vapors and gases, and the transfer of heat. In the back of the book there is a comprehensive subject index.

The book is a practical exposition of the principles of the subject, utilizing experience in teaching and modern methods of presentation.

R. H. OPPERMANN.

MAGNETIC CONTROL OF INDUSTRIAL MOTORS, by Gerhart W. Heumann. 589 pages, illustrations, 15 × 23 cm. New York, John Wiley & Sons, Inc., 1947. Price, $7.50.

This is a subject which is rapidly attaining the specialized stage. Indeed, the application of motor controllers in the most efficient and proper manner often requires extensive knowledge and experience. Control equipment is recognized rightly as the director of motor performance and protector of the operator and the drive. Depending on the work to be done, controllers can be quite complicated and can become parts of integrated control systems involving a multiplicity of rotating and stationary power apparatus. This book is written from the viewpoint of the application engineer and user in treating on what control equipment can accomplish to the end that good judgment can be exercised in selecting the type of control to apply.

At the outset the principles of direct current and alternating current motor operation are given and upon this foundation there is built the discussion of contractors and relays. This leads into descriptions of circuit breakers, control transformers, voltage stabilizers, rectifiers and other equipment which are parts of control equipment. Separately then, there are taken up pilot devices, electronic devices, basic control circuits, amplidyne control circuits, solenoids, thrusters, brakes, intermittent duty controllers, and maintenance of control equipment. One of the most common and most interesting control set-ups in an industry plant is that of the synchronous motor. This is treated quite completely including field application by current-time relay, by slip cycle impedance relay, by slip frequency relay and by timing relay. Field removal is also given attention.

The book has a great many illustrations such as curves, wiring diagrams and photographs to which reference is made and which are very helpful. It is written in a language understandable by the average engineer and is quite complete in coverage. In the back is a subject index which adds considerably to the value of the book as a reference. The book will be useful in the plant engineer's office as a descriptive text.

R. H. OPPERMANN.

ELEMENTS OF ELECTRICAL ENGINEERING, by Arthur L. Cook. Fifth edition, 662 pages, illustrations, 15 × 24 cm. New York, John Wiley & Sons, Inc., 1947. Price, $5.00.

This work is well known to a great many professors and former students as a treatise on fundamentals and their application in practice. There were four editions beginning in 1924 and ending in 1941. During these years considerable advancement was made both in the subject matter and in methods of presentation which necessitated the newer editions. The book at hand is the fifth edition, revised and rearranged.

The first part of 99 pages is devoted to electric and magnetic circuits, giving attention to the electric field, electric potential and current, the magnetic field, its density, hysterisis, induction, capacitance, and the various units involved. With this as a background, Part Two leads into direct current machinery, beginning with a discussion of parts and construction of dynamos, how they operate and what they do. This is an especially good approach, since both theory and practice are covered together. Then there are discussed losses and efficiencies, ratings and guarantees of machines. Control and protective devices are covered separately, followed by a treatment on batteries and systems of direct current transmission and distribution.

Part Three begins the subject of alternating currents, picking up the thread left by Part One. A genuine attempt is made to illustrate clearly the wave form as developed by a rotating

machine, and then transferring this into a discussion on sinusoidal currents and voltages. This section includes the mathematical representation of vectors which is quite well illustrated for the solution of alternating current circuits. The properties of circuits involving resistance, inductance, and capacitance in parallel and in series and the solution of problems using the terms of admittance, conductance and susceptance are thoroughly covered. The final chapter in Part Three is devoted to polyphase circuits. The next part of the book on alternating current machinery starts with a description of the transformer, its physical make-up, vector representations and equivalent circuits. The same method is used with regard to polyphase induction motors, generators, synchronous motors, and synchronous convertors. Single phase motors are taken up separately in similar fashion and the basic types are treated. The rest of this section is devoted to transmission, distribution, switching, protective devices, and motor applications. The last or Part Five of the book, gives a concise but comprehensive treatment of fundamentals and characteristics of electron tubes, the functions and basic circuits of electron tubes and the principles of applications of electronic devices to industry.

This is a plain treatment with many exercises, which if studied diligently and the problems solved, will give a thorough knowledge of electric power machinery.

R. H. OPPERMANN.

THE CHEMISTRY AND TECHNOLOGY OF PLASTICS, by Raymond Nauth. 522 pages, drawings and illustrations, 16 × 23 cm. New York, Reinhold Publishing Corp., 1947. Price, $9.50.

The origin of the plastics industry can be traced back many centuries to the Egyptians and Chinese. As time went on, increasing investigation was made resulting in discoveries, many of which were not put into commercial use because the world was not ready for them. Some plastics like acrylics lay on the shelf for a century before being commercially practical. Today the search for plastics still goes on. As each new material is developed it may serve a particular purpose or have a specific merit, or a particular application. It is possible now to design a plastic material having properties to suit a specific purpose. With this rapid expansion it becomes increasingly difficult to visualize the field of plastics to come.

This book has five sections. The first, on thermosetting resins, has an introduction before discussing various resin compounds falling into this category. Later, attention is given individually to amino resins, thermosetting cast resins, amine-aldehyde resins, the viscous resins, and laminates. Summary data of a general nature appear at the beginning of the second section in the form of tables giving, for well-known types of plastics, adaptability, physical-chemical, and electrical properties, the effect of aging and exposure to light, the coefficient of thermal expansion. This is a fund of information, the location of which in this book can be questioned on the grounds of practical availability for quick reference by those not familiar with the detailed content and plan of the book. The second section on thermoplastic resins covers vinyl polymers and copolymers, and acrylic, polyamide, organic silicon and polystyrene resins. Special attention is given to the grouping of the cellulose plastics in section three, to which there is appended a chapter on regenerated cellulose. Synthetic rubber, natural resins, and plywood are discussed in section four. The last part of this includes veneer processes and molding. The final section of the book, devoted to mold design, presses and equipment, applies the chemical knowledge in the preceding sections to the processes and technology necessary to the finished product.

The book is well written, profusely illustrated, and gives a fund of information on the subject. Diagrams showing relationships and derivations are especially interesting. The appendices and subject index add to the value of the book.

R. H. OPPERMANN.

STEAM, AIR, AND GAS POWER, by William H. Severns and Howard E. Degler. Fourth edition, 509 pages, 15 × 23 cm., tables, drawings and illustrations. New York, John Wiley & Sons, Inc.; London, Chapman & Hall, Ltd.; 1948. Price, $4.75.

The fourth edition of this widely used textbook follows the well-established practices of

the previous editions. It supplies the student of power engineering with the basic information which he will later use in application. The present, revised edition brings the material up-to-date with special attention paid to the gas turbine, the development of which has been unusually rapid within the past ten years.

No significant changes have been introduced in the chapters on steam and internal-combustion engines, although here the subject matter also has been rearranged and further clarified.

H. N. MICHAEL.

BOOK NOTES.

QUANTITATIVE ANALYSIS, by Willis Conway Pierce and Edward Lauth Haenisch. Third edition, 520 pages, 15 × 24 cm. New York, John Wiley and Sons, Inc. Price, $3.75.

Since the second edition of this text was written many changes have been made in the presentation of material to classes and this new third edition, almost entirely rewritten, incorporates these changes. Numerous laboratory exercises have been added and the questions and problems are mostly rewritten and almost doubled in number. The material is presented in four parts: Fundamentals, Volumetric Analysis, Gravimetric Analysis, Special Methods. There are several appendices, which contain useful tables and an index.

W. P.

VIBRATION AND SOUND, by Philip M. Morse. Second edition, 468 pages, illustrations, 15 × 23 cm. New York, McGraw-Hill Book Co., Inc., 1948. Price, $5.50.

In the revision of his work, the author, now director of Brookhaven National Laboratory, has brought up-to-date this important text on the theory of vibration and sound. Wartime developments have been included and the recent advances in the theory of room acoustics have necessitated considerable rewriting of Chapter VIII, Standing Waves of Sound.

In his discussion of the application of operational calculus and the Laplace transform methods to the study of acoustical transients, the author has made a major addition. Besides the new material in the text, the number of problems has also been considerably augmented.

G. E. P.

MECHANICS OF MACHINERY, by C. W. Ham and E. J. Crane. Third edition, 538 pages, illustrations, 16 × 23 cm. New York, McGraw-Hill Book Co., Inc., 1948. Price, $5.00.

This new edition has been revised to include new subjects and bring the material up-to-date. It contains more material than the previous editions, although the same general sequence that was featured in the earlier editions has been retained. The book is divided into two parts. Part One treats mechanism and Part Two, kinematics and dynamics of machinery. The book is arranged in seventeen chapters. Chapter 17 is on the gyroscope, which is new material for this edition. This is followed by an appendix, problems and an index.

W. P.

POPULAR GEMOLOGY, by Richard M. Pearl. 316 pages, illustrations, 14 × 21 cm. New York, John Wiley & Sons, Inc., 1948. Price, $4.00.

Mr. Pearl presents in his book a semitechnical survey of modern gemology. Its eight chapters are systematically arranged and the classifications are based, for the most part, on *Dana's System of Mineralogy*.

The bulk of the work is divided among the first three chapters which deal, respectively, with the recognition of gems, with faceted gems, and with cabochon gems. There are also chapters on silica gems, organic gems (pearls, coral, amber, jet), synthetic gems, and a highly interesting discussion on luminiscent gems.

Jewelers, mineral collectors, and the gem lover in general will find the material discussed in this book authoritative and up-to-date.

H. N. M.

NOTES FROM THE BIOCHEMICAL RESEARCH FOUNDATION.

Manometric Determination of Carboxypeptidase.—CHARLES A. ZITTLE. Carboxypeptidase has been estimated by formol titration with chloracetyltyrosine as the substrate (1). This enzyme retains much of its activity in the presence of formaldehyde and in the procedure mentioned formaldehyde is added at the beginning of the estimation. The amino group of the tyrosine released by hydrolysis is masked by the formaldehyde and the strong monochloracetic acid is readily measured. In the above procedure the acid is estimated by titration at the end of the experiment. This acid also could be conveniently measured manometrically with $NaHCO_3$ present, which would offer the advantage that the acid release could be followed throughout the experiment. The utilization of the manometric procedure is described herein.

EXPERIMENTAL.

Enzyme. The carboxypeptidase was prepared from frozen pancreas by the method described by Anson (1). Preparations of high activity were obtained but satisfactory crystallization did not occur. Recently additional literature on the crystallization of this enzyme has appeared (2,3,4). For the initial assays the precipitate which appears on dialysis was used: 1.0 cc. of a heavy suspension was dissolved with 1.0 cc. of 4.0 per cent NaCl and 1.0 cc. of 0.5 *M* $NaHCO_3$. The concentration was estimated by a nitrogen determination.

Substrate. 0.5 g. of chloracetyl-1-tyrosine was suspended in H_2O, brought into solution with *N* NaOH (about 2.0 cc.) and adjusted to a pH of 9 and a final volume of 25.0 cc. 20.0 cc. of this solution were mixed with 5.0 cc. of 35 per cent C.P. formaldehyde.

Procedure. The following solutions were placed in Warburg flasks: 0.2 cc. of 0.5 *M* $NaHCO_3$, 2.0 cc. of substrate, and water to make the final volume 3.5 cc. including the enzyme which was placed in the side arm. The measured pH was 7.5. The experiments were performed at 37° with an atmosphere of 5 per cent CO_2–95 per cent N_2. The final concentration of substrate was 0.036 *M;* a lesser concentration did not permit a maximum rate of hydrolysis. An experiment was performed in which alanine was introduced into a solution of formaldehyde and dilute $NaHCO_3$; the immediate release of acid, measured manometrically, indicated that the interaction of formaldehyde and amino group was very rapid. A typical experiment with carboxypeptidase is shown in Fig. 1. The rate of hydrolysis was proportional to the amount of enzyme used when readings were taken within the first ten minutes.

The subsequent decline in hydrolysis was probably due to the inhibitory effect of the monochloracetic acid (5) which was formed. The acid group released was sufficiently strong so that it was not completely neutralized by the amino group and it could be measured manometrically without the addition of formaldehyde. The measured acid release,

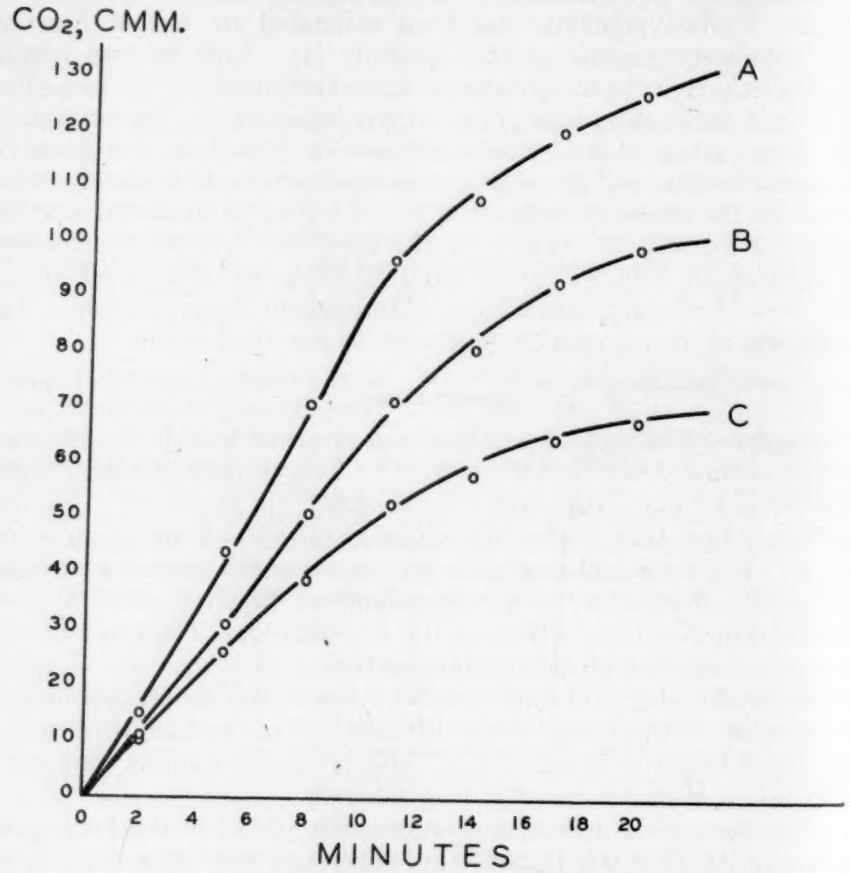

FIG. 1. Hydrolysis of chloracetyltyrosine by carboxypeptidase measured manometrically. The enzyme solution used contained 0.043 mg. N per cc.

Curve A: 0.8 cc. of enzyme solution
Curve B: 0.6 cc.
Curve C: 0.4 cc.

however, was only about 40 per cent as great as when formaldehyde was added.

RESULTS.

In the experiment cited the enzyme which precipitated on the first dialysis of the pancreas extract was used. The activity was 2,600 cmm.

or 0.116 milliequivalent/1.0 mg. N/10 minutes. In the course of the subsequent purification the activity was raised to 0.179 milliequivalent/1.0 mg. N/10 minutes. Anson (1) defined a unit of carboxypeptidase activity as that amount of enzyme which produces 1 milliequivalent of acid in 1 minute. In terms of these units our enzyme contained 0.0179 units/1.0 mg. N. Anson's crystalline enzyme contained 0.081 units/1.0 mg. N. Whether the two methods of estimation give comparable units can only be decided when the crystalline enzyme is available.

DISCUSSION.

The decrease in activity of the carboxypeptidase with time probably is due to the inhibitory effect of the monochloracetic acid (5). Carbobenzoxyglycyl-1-phenylalanine does not have this drawback and it is more rapidly hydrolyzed (5,4). Formaldehyde exerts some inhibitory effect on carboxypeptidase (5) but procedures using it should give satisfactory comparative data.

SUMMARY.

A procedure for the manometric estimation of carboxypeptidase is described.

REFERENCES.

(1) M. L. ANSON, *J. Gen. Physiol.*, **20**: 663, 781 (1937).
(2) J. B. SUMNER and G. F. SOMERS, "Enzymes," 2nd Edition. p. 186. New York, Academic Press (1947).
(3) F. W. PUTNAM and H. NEURATH, *J. Biol. Chem.*, **166**: 603 (1946).
(4) H. NEURATH, E. ELKINS, and S. KAUFMAN, *J. Biol. Chem.*, **170**: 221 (1947).
(5) K. HOFMANN and M. BERGMANN, *J. Biol. Chem.*, **134**: 225 (1940).

CURRENT TOPICS.

Natural Gas Stored in Underground Pipes. (*Compressed Air Magazine*, Vol. 53, No. 8).—Natural gas tapped from fields of the Texas Panhandle and piped nearly 1000 miles by the Public Service Company of Northern Illinois is being stored by the latter in a novel arrangement of buried pipe sections. This method of storage is the first of its kind in the country and originated when the company, faced with the necessity of enlarging existing facilities to meet increased consumer demand, decided to explore the possibility of storing gas underground instead of on the surface in conventional holders. Accordingly, in the fall of 1946, a pilot installation was made at Kankakee, Ill., with a capacity of 1,250,000 cu. ft. The success of this project led to the completion, recently, of a similar system on a 160-acre tract at Mount Prospect, Ill., where 40 million cubic feet of gas is stored underground.

Seamless pipe of high-carbon, molybdenum-alloy steel, similar to that used in the construction of the "Big Inch", was eventually selected. It has an outside diameter of 24 in. and a wall thickness of approximately ½ in. and was made by the National Tube Company of Pittsburgh, Pa. Random lengths were utilized, the average being about 40 ft. Because the high-carbon steel would have been difficult to weld in the field, both ends of each pipe section were forged at the fabricating plant into hemispherical shape and the solid hubs were drilled and tapped to receive 1½-in. threaded connections. After being stress-relieved, the unit was tested hydrostatically at 2800 psi. before being shipped. The volume of each container averages 109.5 cu. ft., the weight 5100 lb., and the capacity 25,000 cu. ft. of natural gas at 2240 psi. pressure.

Of particular interest in this type of storage is the effect of high pressure on the compressibility factor of natural gas. At the operating pressure of 2240 psi., natural gas deviates most from its expected performance, as calculated according to the laws for a perfect gas. Whereas computations indicate that 160 cu. ft. of perfect gas can, under a pressure of 2240 psi., be compressed into 1 cu. ft. of space, it is actually possible with the same pressure to force 230 cu. ft. of natural gas into the same space. This behavior of natural gas increases the capacity of the pipe sections by some 40 per cent, permitting the storage of much more gas than their actual volume would seem to indicate.

As the compressibility factor of natural gas becomes increasingly favorable with decreasing temperature, it is desirable to bury the pipe at a depth that will give reasonably low temperatures in winter and yet minimize seasonal changes. At 2240 psi. pressure, each 1°F. variation in temperature causes a pressure change of about 10 psi., one half of which is attributable to the change in the compressibility factor that accompanies the temperature change. Owing to seasonal temperature variations, some gas must be withdrawn from storage in spring and summer and a corresponding amount put back in fall and winter.

R. H. O.

The Transistor—A New Amplifier. (*Electrical Engineering*, Vol. 67, No. 8)—A new type of amplifying element known as a "transistor" which promises to

have far reaching significance in electronics and electrical communication was demonstrated recently before members of the press by the Bell Telephone Laboratories, Inc., New York, N. Y. Like a vacuum tube, the transistor can serve as an amplifier or as an oscillator, yet it contains no vacuum, glass envelope, grid, plate, or cathode.

Two point contacts of the "cat's whisker" or detector type are made to a semiconductor (germanium was used in the samples demonstrated) 0.002 in. apart. The entire apparatus is housed in a small metal cylinder less than an inch long. The unit has been shown to produce amplification as high as 100 to 1 (20 decibels), and some test models have been operated as amplifiers at frequencies up to ten megacycles.

A number of interesting applications for the transistor were presented. In one demonstration it was used to amplify audio frequencies traveling between two telephones. In another, a tubeless radio receiver using transistors as amplifiers, and a point contact rectifier for a detector, was operated satisfactorily. A transistor also was used to generate a standard frequency tone, thus demonstrating its capability as an oscillator.

The transistor is said to be little affected by ordinary changes in temperature (−50 to +50°C.), and such characteristics as life, ruggedness, and stability are expected to be much the same as those of point contact rectifiers though no data are available at the present time. Because the device is still in the experimental stage no data on cost are available either.

Electrically, the transistor differs somewhat from the ordinary vacuum tube. The input impedance is low (about 1,000 ohms) and the output impedance is high (about 10,000 ohms). The power handling capability of the units demonstrated was 50 milliwatts, and the power consumption is about 0.1 watt.

The amplification process in the transistor is caused by the fact that the input contact (called the "emitter") is surrounded by an "area of interaction." Within this area the electronic structure of the semiconductor is modified by the input current. If the output contact (called the "collector") is placed in this area, the output current can be controlled by the input current thus producing the basic mechanism of amplification.

R. H. O.

Silver Reclaiming Kit.—Gopher Laboratory, Minneapolis 1, Minn., now has available a Silver Reclaiming Kit designed especially for users of hypo in small quantities.

Active material is the same as that in the large Silver Reclaiming Cartridge Units, which have been in use by many large commercial photofinishers the past two years.

The Kit consists of 50 Silver Reclaiming Filaments, each of which will reclaim the silver from ½ gal. of film or X-ray hypo, or 1 gal. of print or photostat hypo.

The process is very simple, and merely consists in dropping one or more Filaments into the container of exhausted hypo, and allowing to stand overnight. The next day the hypo is poured off, and the silver-covered Filament lifted out. When the entire Kit has been used, the dried Filaments are sent to the Laboratory for refining. Upon receipt, the user is paid 100 per cent of the silver value, minus refining charges.

The Kit sells for $1.50 and will reclaim up to $15.00 worth of silver.

Steam Pipes for Hottest Turbine to Run Dull Red.—The 100,000-kw. turbine recently shipped by the Westinghouse Electric Corp. for installation at the Sewaren Generating Station of the Public Service Electric and Gas Co. of New Jersey will operate at such high temperatures and pressures that the steam pipes feeding it will glow a dull red. Steam at 1500 lb. pressure and 1050°F. will feed the new 3600-rpm. tandem compound double flow machine. This is the first steam power plant to be constructed for operation under such conditions.

While the highest temperature previously used in turbines is 1000°F., it is the last 50°F. that makes the job tougher. To withstand operating in the dull red region steam containers such as the throttle valves, steam chests and other high pressure parts of the turbine are constructed of 18–8 stainless steel. Fabrication of parts from this hard-to-work material has been a problem in itself.

The importance of the 50° rise in temperature is in the fuel savings. For each 50° increase, the quantity of coal required to produce one kilowatt hour of electrical energy is decreased by about 1.4 per cent. In 1915 the output of all our steam power plant turbines averaged only 525 Kwh. per ton of coal burned. With further developments towards increased plant efficiency, the output of all steam power plants by 1945 was 1550 Kwh. per ton of coal burned. These figures include both old and modern plant equipment in service during the year mentioned. This new turbine will produce about 2500 Kwh. of electrical energy from each ton of coal burned.

Gas Turbine for Electric Utility.—The first gas turbine for an electric utility in this country is under construction at the General Electric Company's Schenectady Works and will be shipped to the Southwest early in 1949.

A duplicate of the 4800-hp. locomotive gas turbine now undergoing tests, the 3500-kw. turbine generator set was purchased by the Oklahoma Gas and Electric Co. It will be installed at the Arthur S. Huey station, Oklahoma City.

The new gas-fired unit will be installed in an extension to the present station and operated on natural gas which is available in abundance in the area. The waste heat from the exhaust will be used with a separate heat exchanger to supplement the present boiler feed water heating system. This will result in additional kilowatt output from the station by releasing part of the heating load from the present installed equipment.

The "straight-through" or in-line arrangement of the compressor, combustion chambers, and turbine was selected for this application. It has been designed for long life and low cost fuels.

Because there are only two major moving parts, the turbine and compressor rotors, maintenance of the gas turbine is expected to be low.

The unit has been designed for maximum accessibility during maintenance and inspection periods, elements such as combustion chambers which might normally require maintenance being easy to replace.

The new gas turbine will be geared to a conventional 3600-rpm. totally enclosed generator with direct connected exciter. The only water required in the operation of the plant will be a small quantity for cooling the bearing lubricating oil and for cooling the a-c. generator.

R. H. O.

Operation Bootstrap.—The importance of "Operation Bootstrap," a means for producing a new atomic fuel while other atomic fuel is consumed making useful power, was emphasized by Bruce R. Prentice in a paper presented recently to the Pacific Convention of the A.I.E.E. Mr. Prentice spoke on "Design Criteria for Atomic Power Reactors."

"Perhaps the most important criterion of a major atomic power plant of the future will be its ability to 'breed' more new fuel than it burns," Mr. Prentice said. He also said that such an atomic plant, instead of just using up the world's supply of fuel as is done in ordinary fuel plants, would add to the world's supply at the same time it released useful energy.

"Of course, we never get something for nothing," Mr. Prentice pointed out, "and here the newly created fissionable material comes from the non-fissionable 'source material' uranium 238 or from thorium. However, neither of these is now fissionable or useful as fuel and they are vastly more abundant than the only natural atomic fuel, rare uranium 235. So in a very real sense, breeding will be a 'bootstrap' proposition of getting new fuel while burning other fuel making power."

Mr. Prentice hastened to emphasize caution in guessing when such a "breeder atomic power plant" might be a practical reality. He said that at present it looks theoretically possible and it may be demonstrated experimentally in two or three years. "Will atomic power be ours in 1965, 1975, or 2000?" he asked. He concluded that the answer will depend on future developments in technology, economics, politics, and international relations.

R. H. O.

70-Million Volt Synchrotron.—A 70-million-volt synchrotron, a type of atom smasher, is being built for Queens University, Kingston, Canada.

Under construction in General Electric's General Engineering and Consulting Laboratory, the machine will be used by the Canadian institution for nuclear research.

Newest among the "particle accelerators," as atom smashers are known to nuclear physicists, the synchrotron, like the betatron, accelerates electrons. There are significant advantages in this new type, particularly for the development of higher voltage machines.

Basic feature of the synchrotron is the principle of "phase stabilization" it employs. This means that accelerating electric impulses occur at exactly the right time to boost electrons as they circulate in the machine's vacuum doughnut, or acceleration chamber. The tendency for automatic synchronization gives rise to the name "synchrotron."

Although this electro-nuclear device utilizes an electro-magnet, the main acceleration is provided by an electrostatic field. When electrons have been accelerated by magnetic induction to an energy of 2,000,000 electron-volts, and are traveling at 97 per cent of the speed of light, a radio frequency oscillator turns on automatically. The oscillator is connected to a gap on the inside of the synchrotron doughnut, and circling electrons receive an increase in energy each time they go past.

At a predetermined time the path of the electrons is altered slightly so that they strike a small piece of metal inside the doughnut, producing an X-ray

beam. These X-rays are many times more penetrating than those produced by conventional X-ray machines, or by radioactive substances such as radium.

Queens University's Prof. J. A. Gray and his collaborators, Dr. H. M. Cave and Dr. D. T. Roberts, together with other Canadian scientists, will employ the machine to conduct research with high-energy X-rays. The synchrotron will be installed in a special underground chamber to protect personnel from harmful radiations, and will be operated from a remote-control station in a nearby building.

R. H. O.

Special Committee on Technical Information Formed.—Formation of a Special Committee on Technical Information to promote effective exchange of research and development information among the departments of the National Military Establishment was announced recently by Dr. Vannevar Bush, chairman of the Research and Development Board, National Military Establishment.

The committee will study the problem of collecting, correlating, reproducing and disseminating technical information potentially useful in the research and development program of the National Military Establishment. Study and application of new methods and techniques to the problem of technical information organization, and promotion of active research in this effort, are expected to receive especial attention by the group.

At the first meeting of the committee, Dr. Detlev W. Bronk, chairman, pointed out the desirability of applying scientific methods to utilize more effectively the large body of information created by scientific activity.

"The handling of results of research in the matters of publication, dissemination and assimilation has not in the past shown an experimental or adventurous approach," Dr. Bronk stated.

Membership of the Special Committee on Technical Information includes: Professor John E. Burchard, Dean of Humanities, Massachusetts Institute of Technology; Herman Henkle, Director of the John Crerar Library; Lt. Col. F. L. Walker, Jr., Army; Captain W. H. Leahy, Navy; Colonel Bernard A. Schriever, Air Force. Norman T. Ball is executive director of the committee.

Symposium on Steroid Hormones.—A phase of science which had its roots at the University of Wisconsin returned to the university as a growing, important branch of life study at the University Centennial Symposium on Steroid Hormones, held in September.

Back in 1927, a Wisconsin scientist, Dr. Frederick L. Hisaw, began isolating chemical compounds he found in animals and people which he thought bore some relation to health.

This week, scientists from all over the world gathered at Wisconsin and confirmed his basic assumptions. They spent three days exchanging information on the findings they made—findings which indicate that these chemical compounds, complicated in structure, fatty in nature, and made for the most part in glandular organs, actually play a major part in the chemical processes of life, health, and disease.

They reported that they have isolated 56 different steroid compounds in human urine, but as one of the scientists pointed out, "we're not completely certain of the origin, the function, or the real importance of most of them."

Among the better known steroid hormones they listed vitamin D, morphine, bile acids, and cholesterol. It is cholesterol, the most abundant of all steroid compounds in animal tissue, which is the parent substance for all other steroids, they said.

Most of the work done thus far, the symposium of 600 experts in the field revealed, has been done on two of the chemical compounds, the male hormone and the female hormone.

The Symposium on Steroid Hormones was the third symposium in the University of Wisconsin's Centennial series. It was supported by funds through the university by the Wisconsin Alumni Research Foundation, and from the National Research Council Committee on Growth, acting for the American Cancer Society.

Dr. W. S. Gordon, chairman of the symposium arrangements committee, reported on the conclusion of the symposium: "It has crystalized ideas in this important field, and brought us all up-to-date on each other's work. Unfortunately, it vividly illustrated how much more work must be done in the field, too."

Exposure to Air Improves Some Wyoming-Type Bentonite.—New information about bentonite, a clay mineral used chiefly in the foundry and petroleum industries, has been uncovered according to an announcement made recently by Geological Survey Director W. E. Wrather.

Studies of Wyoming-type bentonite by Margaret D. Foster, Survey Geochemist, have revealed that the blue-gray subsurface material, now rejected in mining because of a deficiency in the necessary colloidal properties, becomes similar to high-grade material in important respects if permitted to oxidize. This blue-gray material is identical in chemical composition and iron content with the green near-surface bentonite now being mined, but it was found that the iron in the blue-gray material is predominantly in the unoxidized or ferrous state, whereas in the green material the iron has been oxidized to ferric iron, as previously suggested by M. M. Kenchtel of the Geological Survey.

The swelling test, one of the criteria by which the colloidal properties of bentonites are judged, indicated that the blue-gray material swelled or expanded in water only two-thirds as much as the green. It was found, however, that the iron in the blue-gray material oxidized relatively rapidly on exposure to air and that the swelling property also increased correspondingly. After ten months' exposure the iron in the blue-gray material had reached the same state of oxidation as that in the green material. At the same time the swelling property had increased also and had become equal to that of the green material.

This information should be of considerable value to those interested in mining the Wyoming-type bentonite because it suggests that by simple processing the blue-gray material now rejected might be converted to usable bentonite. Researches on the problem are continuing.

What's New in Equipment (*Factory Management and Maintenance*, Vol. 106, No. 9).—(1) Electrical wire with rubber insulation that is said to improve when soaked in water was developed for use underground and in locations where high moisture resistance is required. Wire is coated with natural rubber latex compound, called Laytex RUW, applied by the dip process. (2) Thermo-

plastic matting is suitable for use where acids or oils are present, or in locations where matting is given rigorous service. Manufacturer says it will lie flat and hug the floor. Manufactured in black and brown, it is 3/32 in. thick by 36 in. wide and comes in rolls 25 to 35 yards long. (3) Suitable for marking storage bays, aisles, stock locations, equipment clearance limits, and traffic lanes, marking paint is heavily based with fine silica, making it non-slippery. It comes in white and yellow, in 1- and 5-gal. cans. Manufacturer states that it resists strong cleaners, and retains its color and visibility after repeated scrubbings.

Czech Builds Road-Type Gas-Turbine Engine (*Product Engineering*, Vol. XIX, No. 9).—A Czech engineer, George Lakes, now working in the car repair shops at Hameln, in the British Zone of Germany, has become another entrant in the race to design a gas turbine for road vehicles. His engine is built from scrap; his only tool was a 6-in. lathe.

Apparently, Lakes' engine (about 150 hp.) combines, as the propulsive force directed into the turbine, a mixture of steam and burnt-fuel gas, at a maximum temperature of 985 F. The exhaust gas mixture is cooled in an air-cooled condenser, which should mean there is no heat-exchanger. Speed of rotation is 13,000 rpm. Calculated potential thermal efficiency is 20 to 30 per cent; thermal efficiency of the rough prototype is figured as only 5 per cent.

Line Shot Blast Room with Rubber. (*The Foundry*, Vol. 76, No. 9).—Installation of an abrasion resisting rubber compound on the walls and ceiling of its shot blast room solved a tough maintenance problem for a New England manufacturer of textile machinery. Two-inch wooden planking formerly lined the room, and under the punishment of shot from the hose against the rough castings, its ordinary life was about one month. It then had to be replaced, and the room shut down until the maintenance job was completed.

Since the $\frac{1}{4}$-in. fabric backed rubber compound manufactured by the B. F. Goodrich Co. was installed in May, 1947, there has been no maintenance problem and the installation shows no appreciable wear, according to the rubber company.

Quick Starting House Turbine-Generator Unit.—A 6000-kw. General Electric house turbine-generator unit designed for quick starting and capable of picking up full load instantly has been installed at the Pacific Gas and Electric Company's Kern Steam Plant near Bakersfield, Calif.

Under normal operation, the turbine floats on the line, carrying load in accordance with the steam demand of the deaerating heater of the main unit and exhausts through a 5-lb. extraction opening.

In case of a disturbance in the electrical system, the house turbine generator is automatically isolated from the main bus and picks up the entire station auxiliary load instantly.

The 6000-kw. turbine-generator is capable of going from a cold standstill to full speed and full load within 20 sec. with steam 1350 lb. gage and 950° F. total temperature. Extensive factory tests of the complete unit proved its capabilities for the unusual service for which it was designed.

Although designed for quick-starting, the unit is expected to be in operation practically all the time.

R. H. O.